

# Fire Technology

## Advanced modeling of composite slabs with thin-walled steel sheeting submitted to fire --Manuscript Draft--

<b>Manuscript Number:</b>	FIRE469R1
<b>Full Title:</b>	Advanced modeling of composite slabs with thin-walled steel sheeting submitted to fire
<b>Article Type:</b>	Manuscript
<b>Keywords:</b>	fire resistance, composite slabs, numerical modeling
<b>Corresponding Author:</b>	Euripidis Mistakidis University of Thessaly Volos, GREECE
<b>Corresponding Author Secondary Information:</b>	
<b>Corresponding Author's Institution:</b>	University of Thessaly
<b>Corresponding Author's Secondary Institution:</b>	
<b>First Author:</b>	Daphne Pantousa, Civil Engineer, MSc
<b>First Author Secondary Information:</b>	
<b>Order of Authors:</b>	Daphne Pantousa, Civil Engineer, MSc Euripidis Mistakidis
<b>Order of Authors Secondary Information:</b>	

### DETAILED RESPONSE TO THE COMMENTS OF THE REVIEWERS

The authors would like to thank the anonymous reviewers for their constructive criticism and their valuable comments. Following are the detailed responses to the comments of the reviewers.

On behalf of the authors,  
Prof. E. Mistakidis

#### **ANSWERS TO THE COMMENTS OF THE 1st REVIEWER**

**REVIEWER'S COMMENT:**

In general, this is a reasonable paper which offers quite a simplified yet logical approach to fire design of composite slabs. However, there are big short-comings in the sense that neither of the models presented (simplified or advanced) have been validated and they cannot be directly compared. Also, even in the qualitative comparison, the results for the simply supported and continuous slab are quite different (different model is more conservative in each case).

I would suggest that the author ought to validate their approach against available FE analysis and test results. See the information and references in the following papers:

1. **Cashell K.A.**, Elghazouli A.Y. and Izzuddin B.A. (2011). "Failure Assessment of Lightly Reinforced Floor Slabs. I: Experimental Investigation", ASCE Journal of Structural Engineering Volume 137, pp 977-988.
2. **Cashell K.A.**, Elghazouli A.Y. and Izzuddin B.A. (2011). "Failure Assessment of Lightly Reinforced Floor Slabs. II: Analytical Studies", ASCE Journal of Structural Engineering Volume 137, pp 989-1001.

The advanced numerical model has now been validated against published experimental results (reference [14] of the revised version). The corresponding study is included in the Appendix.

**REVIEWER'S COMMENT:**

Also, the comments below should be considered before publication:

(i) Membrane behaviour in the slab is not mentioned in the paper. As the temperature increases and the deflections increase, the load-carrying of the slabs (both simply-supported and composite) will increase accordingly. Although this is implied in the paper (increasing moments) it should be explained more explicitly as these are terms common to fire design of slabs.

The membrane action is not mentioned in the paper because in both static systems, the slab is free to expand in the axial direction and subsequently no axial forces arise.

**REVIEWER'S COMMENT:**

(ii) At no point is slippage between the steel deck and the concrete slab been discussed, or the effect that this may have on load carrying capacity. Bond-slip has been shown to be a very important factor in the ultimate capacity of slabs.

The typical failure mode for fire exposed composite slabs is the flexural failure. The longitudinal shear failure is typical for ambient conditions. According to experimental results that are presented in [14] and [22], this kind of failure has not been observed under fire conditions. This can be attributed to the fact that the temperature of the steel decking increase rapidly during the fire. The steel decking loses its strength and the tensile forces are undertaken from the reinforcing bars. Therefore, longitudinal shear failure does not seem to be a critical phenomenon during the fire exposure. A comment was added in page 15 for clarification.

REVIEWER'S COMMENT:

(iii) It has been shown in other studies on composite slabs in fire that the steel deck debonds from the concrete slab at around 400 degrees. Was this shown in the FE analysis in this paper?

The phenomenon mentioned by the reviewer has been observed in fire tests as it is reported in [14] and [21]. However, as it is stated in [14], the phenomenon is local and was observed in composite slabs with steel sheeting of considerable height. Therefore, a perfect bond between the steel decking and the concrete is assumed in the advanced numerical model presented in the present paper. This assumption has also been adopted by several former numerical studies (see [5], [14], [23] etc). A comment was added in page 15 for clarification.

REVIEWER'S COMMENT:

(iv) Was an initial gravity load applied to the slabs (in the numerical model) before the temperature was applied? This would affect the deflections.

Yes, the initial gravity load is applied before the temperature starts to increase. A comment was added for clarification in section 5.3 (page 17).

REVIEWER'S COMMENT:

(v) Had the advanced FE model been validated? It is a shame that the simplified model and the advanced model can not be directly compared. This is a failing in the paper as neither model has really been validated.

The validation is included in the Appendix of the revised version.

REVIEWER'S COMMENT:

General comment:

The 'Introduction' section of the paper goes through existing models which have been developed to predict the behaviour of slabs in fire. However, the most recently proposed model has been omitted – see reference 2 above.

A small paragraph was added in the introduction section (Pages 2-3) and the appropriate reference was added.

## ANSWERS TO THE COMMENTS OF THE 2nd REVIEWER

### REVIEWER'S COMMENT:

#### General comments

1. The objective of this article is very practical, as the full-scale fire resistance tests are very expensive and I believe the numerical method for testing the fire resistance of material will be a more accurate and important way in fire protection engineering.
2. The methods used in this research are very clearly explained. The design of the methods for different cases may be different, but the author is able to make the reader follow the methods in a good way. The graphs and tables are very clear useful in order to understand the results of different methods.
3. The different methods give very different results. The author is able to clearly analyze what the reasons are. This makes the comparison between different methodologies (though based on different theories) more meaningful and practical.
4. Main discussions are clearly explained with some exceptions as seen on page 20 : *“the simplifications introduced by the Eurocode 4 with respect to the calculation of the temperature of the components of the composite slabs were assume to be piece wise uniform across the depth of the slab “this assumptions is not correct which lead to some differences in the bending moment resistance that are calculated by the two methods”* This is quite confusing and there are no more reference throughout the paper that prove this.

Figure 3 illustrates the temperature distribution in the cross section of the slab according to EC4. It can be observed that the temperature is assumed to be uniform along the horizontal zones of concrete and for the different parts of the steel sheeting (upper flange, web and lower flange). The temperature distribution that results from the thermal analysis, (as it is illustrated in Figure 14) indicates that this assumption is not so realistic.

The paragraph was corrected in the following way (page 21):

“Following the code, the temperatures were assumed to be uniform along the horizontal zones of the concrete. Moreover, each part of the steel sheeting (upper flange, web and lower flange) is supposed to have a uniform temperature. The above are illustrated in Fig. 3.”

### REVIEWER'S COMMENT:

#### Typo:

#### 1. Typos - Space between number and unit

P7 line 10-11 3.5m-> 3.5 m

P7 line 13 7m -> 7 m

P7 line 15-16 3.97KN/m<sup>2</sup> -> 3.97 KN/m<sup>2</sup> 5KN/m<sup>2</sup> -> 5 KN/m<sup>2</sup> (and several more on page 7.)

P8 line 50-51 The mechanical properties used in the calculation, -> The mechanical properties are used in the calculation (are is missing )

P13 line 15-16 300C ->300 C

P13 line 44-45 187.5mm -> 187.5 mm

P13 line 53-54 1.75m -> 1.75 m

P16 line 24-25 20C ->20 C

P16 line 51-52 180C -> 180 C

P18 line 19-20 204mm -> 204 mm

P18 line 36-37 9.07mm/min -> 9.07 mm/min

P19 line 30-31 77mins -> 77 mins

P19 line 48-49 170mins -> 170 mins

P20 line 8 1101C -> 1101 C

P21 line 20-21 152mins -> 150 mins

P2 line 17-18 : the well know -> n is missing for known

P1 line 14-15 : There is no period at the last part of the sentence.

P10 line 36: In this case -> In this case, ( comma is missing? )

P13 line 20-21 : because the negative moment due the external loading is -> because the negative moment due to the external loading ( to is missing )

P19 line 31-32 67<sup>th</sup> minutes -> 67<sup>th</sup> minute

P20 line 20-21 : may lead to some differences in the in the bending -> may lead to some differences in the bending ( double in the )  
In Figure 4. The dashed line should be corresponding to  $M_{ft.Rd}$  instead of  $M_{ft.Sd}$  (mentioned on page 10, section 4.2)

The typographical errors were corrected.

REVIEWER'S COMMENT:

**Unification of words**

mins or minutes ?? (It would be better if the same term is used in the paper)

The term mins was replaced by the word minutes all over the text and figures.

REVIEWER'S COMMENT:

**Specific comments**

VALIDITY

**Data: Are data sources specified and are they valid sources for the author's purpose? Are uses of subjective judgments clearly identified, appropriate, and developed according to an explicitly described logic?**

Starting from table 1 all data sources are clearly identified from reliable sources as the Eurocodes. For instance, Moment diagrams are constructed and are made equal to the resistance moment so that equilibrium is satisfied. The maximum momentums are compared in page 12 mentioning the ultimate load resistance that has a direct impact in the overall results. The judgment in this paper is also clearly identified "*The change between statically undetermined and determined simplifying the calculations because the temperature gradient has no effect on the bending moments that develops*". Therefore the temperature increment can be easily calculated.

Graphic of the different bending moments help clarify the author's equation and assumptions as shown in figure 7. All judgments are clearly identified and are followed accordingly by the described logic used thought the paper. All moment diagram are shown in figure 8 and explained in page 12.

No specific comment for corrections was given.

REVIEWER'S COMMENT:

**Assumptions: Are all significant assumptions explicitly stated? Are there other assumptions not explicitly considered but which also may be reasonable? If some conditions could change the conclusions, are they indicated? Are the assumptions unusual in any important respects?**

Pg13Ln48 Whether the author could describe the effect of this simplification. Just a sentence like "such simplification would lead to the same result as the full scale analysis", or like the way the author did in Pg17Ln22 for convective heat transfer coefficient.

The following sentence was added (page 14):

"These simplifications will not affect the results, which will be identical with those of the full model"

REVIEWER'S COMMENT:

**Methodology: Are experimental, statistical, or other mathematical procedures clearly identified? Are the procedures appropriate and are they applied correctly?**

In Pg3Ln30 the author claimed that the comparison is made to assess the effectiveness of the simplified model based on the proposal of Eurocode4. It would be more convincing if the author could refer to some experimental result or more cases could be done to prove that the advanced model developed by the author could produce more accurate result.

In the revised version the numerical model has been validated against experimental results. The corresponding study is included in the Appendix.

REVIEWER'S COMMENT:

In Pg11, the delta temperature steps were set at 5 °C. However, there are no explanations for this value. It can be inferred that this step is base in an expectancy of a small error uncertainty in the measurements and that any lower value will have no direct impact in the final results.

The following sentence was added in page 13:

"The above procedure was applied with a temperature step  $\Delta T = 5^{\circ} C$ . After parametric studies it was concluded that this value provided a good balance between accuracy and efficiency."

REVIEWER'S COMMENT:

**Results: Do the assumptions and analyses logically support the results and conclusions? If the results are counter-intuitive, has this been addressed?**

In Pg15Ln48 to Pg16Ln8: It would be better to specify if the factors, mentioned as demanding tasks, reduce the credibility of the simulation significantly. If not, it may be better to have explanation of what percentage of the credibility is reduced approximately

The mentioned nonlinear effects were taken into account during the analysis. The following sentence was added in page 17:

"In the present paper, the behavior of the composite slab in elevated temperatures is modeled through combined thermal-mechanical analysis which takes into account all the aforementioned non-linear effects."

REVIEWER'S COMMENT:

**Credibility: Are appropriate references given? Are known facts and situations represented correctly? Are special cases considered?**

Some drawbacks are specified with respect to reinforce concrete slabs. "*It loses quickly its mechanical properties*". However, some values are not explained for example in page 8 the value for the partial safety factor is not explained where it was obtained.

The sentence in page 8 was completed as follows:

"The combination factor  $\psi_{1,1}$  is considered here equal to 0.5 according to the Eurocode 0 [21]. This value corresponds to the building categories A and B i.e. domestic areas or offices."

The corresponding reference for Eurocode 0 was added.

REVIEWER'S COMMENT:

USEFULNESS

**Output: Are the results presented in useful form, with conclusions spelled out so that they are meaningful to the reader? Will the results improve fire safety decision-making?**

In the method presented in this paper, an algorithm is introduced, that facilitates the determination of fire resistance time. The fire resistance time determined accordingly to this criterion is in rather good agreement with the one calculated through the simplify model. As seen in table 4. It would be reasonable to better use the simplified model rather than the complex one. Comparing the result the tables [1, 2, 3, 4] for the fire resistance time, there is a 10 minutes difference between the two methods which does not help the decision making. It is advisable to use a safety factor and it would make more sense to still use the Eurocodes and the current methods.

For sure, for design purposes, the Eurocodes should be followed. However, it is the objective of the paper to assess the validity of the approaches introduced by the codes.

REVIEWER'S COMMENT:

**Limitations: Are the limitations of the methods and data pointed out clearly and candidly? Are the conditions under which results and conclusions can be applied identified and explained?**

For the case of the continuous slab, the fire resistance rating depends strongly on the applied criterion. And accordingly it is this one related to the deflection. Though, there is no more information concerning this relation in the conclusion. "*It has to be noticed first that a direct comparison between the simplified and advanced model is not possible, because the fire resistance in the simplified models is defined though*"

*attainment of the ultimate strength of the structural system, whereas the simplified method is defined through maximum deflection rates".* This last paragraph is quite confusing and counter- intuitive.

The reviewer is absolutely right. The paragraph was modified as follows (page 20):

"It has to be noticed first that a direct comparison between them is not possible, because the fire resistance in the simplified models is defined through the attainment of the ultimate strength of the structural systems while in the case of the advanced models the fire resistance is defined through maximum deflections or deflection rates. However, some qualitative comparison is still possible."

# Advanced modeling of composite slabs with thin-walled steel sheeting submitted to fire

Daphne Pantousa<sup>1</sup> and Euripidis Mistakidis<sup>2</sup>

<sup>1</sup>Civil Engineer, MSc, Doctoral Candidate

<sup>2</sup>Professor of Structural Analysis

*Laboratory of Structural Analysis and Design, Dept. of Civil Engineering, University of Thessaly, Pedion Areos, 38334 Volos, Greece*

e-mail: [emistaki@uth.gr](mailto:emistaki@uth.gr), +302421074171

**Abstract.** The paper studies the behavior of composite slabs with corrugated steel sheeting at elevated temperatures. Two structural systems are considered: a simply supported composite slab and a continuous composite slab that consists of two equal spans. Both of them are designed according to the respective Eurocodes to have similar strengths at room temperature. In the sequel, sophisticated three-dimensional models of the slabs are developed. Coupled thermo-mechanical analysis is used, which takes into account the various nonlinearities that are present in the physical model (dependence of the thermal and mechanical properties of the material on temperature, nonlinear material behavior, cracking etc). The results of the thermal analysis are compared with the temperature field that is proposed in Eurocode 4. For both the structural systems, the fire resistance, in time domain, that yields from the coupled analysis is compared with the fire resistance that results following the provisions of Eurocode 4. Another objective is to evaluate the effect of static indeterminacy on the fire resistance of composite slabs.

**Keywords:** *fire resistance, composite slabs, numerical modeling.*



# Thermo-mechanical modeling of composite slabs with thin-walled steel sheeting submitted to fire

**Abstract.** The paper studies the behavior of composite slabs with corrugated steel sheeting at elevated temperatures. Two structural systems are considered: a simply supported composite slab and a continuous composite slab that consists of two equal spans. Both of them are designed according to the respective Eurocodes to have similar strengths at room temperature. In the sequel, sophisticated three-dimensional models of the slabs are developed. Coupled thermo-mechanical analysis is used, which takes into account the various nonlinearities that are present in the physical model (dependence of the thermal and mechanical properties of the material on temperature, nonlinear material behavior, cracking etc). The results of the thermal analysis are compared with the temperature field that is proposed in Eurocode 4. For both the structural systems, the fire resistance, in time domain, that yields from the coupled analysis is compared with the fire resistance that results following the provisions of Eurocode 4. Another objective is to evaluate the effect of static indeterminacy on the fire resistance of composite slabs.

*Keywords: fire resistance, composite slabs, numerical modeling.*

## 1. Introduction

Composite slabs made with corrugated steel sheeting are commonly used nowadays for the covering of large spans. With respect to ordinary reinforced concrete slabs, they exhibit a number of advantages, as e.g. the ability for the casting of concrete without additional scaffold structures, ease of construction etc. However, concerning fire resistance, they exhibit a significant drawback with respect to reinforced concrete slabs, due to the fact that the corrugated steel sheeting may be directly exposed to fire and, consequently, lose quickly its mechanical properties (stiffness and strength degradation). For this reason, additional reinforcement is usually used in order to ensure that the slab will retain its robustness for the amount of time required by the various fire design codes.

The last decades the research on the fire behavior of composite slabs is focused mainly on experimental studies. A lot of fire tests have been conducted in order to study the fire behavior of composite slabs as individual structural members [1], [2], [3], [4]. The most important full scale fire tests, in terms of understanding the structural behavior of composite slabs, were carried out in the Cardington laboratory in the UK. The later tests indicated that the steel-concrete slabs have an important contribution to the prevention of the collapse of the structure. Since the fire tests are

1  
2  
3  
4 very expensive, the research nowadays is usually carried out through numerical methods.

5  
6 Various research studies referred to the Cardington fire tests, used numerical simulations in order  
7  
8 to determine the fire performance of the slabs (see e.g. [5], [6]).

9  
10 For the numerical simulation of the behavior of composite slabs, various models have been  
11  
12 proposed in the literature. A numerical model was proposed in [6] in order to predict the fire  
13  
14 performance of orthotropic composite slabs. For this purpose a layered slab element was used in  
15  
16 order to simulate the concrete. The steel reinforcement was modeled through a smeared steel  
17  
18 layer. The numerical analysis was conducted with the well-known software package Vulcan [7].

19  
20  
21 A model for the simulation of an orthotropic slab in fire was proposed in [8], which was again  
22  
23 developed within the software code Vulcan. In order to obtain the real temperature distribution  
24  
25 within the slab, the upper continuous portion of the profile was modeled through layered  
26  
27 isoparametric slab elements. In this respect the temperature of each layer of the slab was not  
28  
29 necessarily uniform in the horizontal plane and it was assumed that temperature can vary  
30  
31 between different Gauss integration points. A frame element was used to represent a group of  
32  
33 ribs of the slab. The width of this element was an “equivalent” width, calculated from the  
34  
35 geometric properties.

36  
37 A finite element analysis of the first Cardington test was carried out in [9]. In particular, three-  
38  
39 dimensional shell elements were used to model the behavior of the composite slab, which took  
40  
41 into account material and geometric non-linearity, as well as curvature and non-linear thermal  
42  
43 gradients. This work underlines the effects of thermal expansion during the fire exposure. A  
44  
45 more accurate thermal analysis of composite slabs was performed in [10], where a finite element  
46  
47 adaptive heat transfer program was used. This model took into account the temperature  
48  
49 differential between the hot steel metal deck and cold concrete, as well as the air gaps that arise  
50  
51 between the materials. This problem was modeled using interface elements between the concrete  
52  
53 and the steel profile.

54  
55 Finally, the failure assessment of lightly reinforced floor slabs under elevated temperature is  
56  
57 investigated in [11]. Both a finite element model and a simplified one are developed in this  
58  
59 study. The finite element model uses a special 2D shell element implemented in ADAPTIC,  
60  
61

1  
2  
3  
4 while the simplified analytical model takes into account the influence of bond between the steel  
5 reinforcement and concrete. The validity of the models is examined through the appropriate  
6 validation against experimental results.  
7  
8  
9

10  
11 In the present paper a numerical model is developed to assist the evaluation of the behavior of  
12 composite slabs in elevated temperatures, which is based on the coupling of three-dimensional  
13 solid elements that model the concrete with 4-node shell elements that model the steel profile.  
14 Reinforcing steel bars are modeled through three-dimensional frame elements. The model is able  
15 to take accurately into account the effects of the increased temperature. The temperatures in the  
16 corrugated steel sheeting and in the mass of the slab are calculated by considering accurately the  
17 parameters that affect the thermal problem. The thermal loading is applied on the lower side of  
18 the slab and follows the standard ISO 834 fire curve adopted by Eurocode 1 [12]. The thermal  
19 and structural material properties in elevated temperature are taken into account according to the  
20 respective Eurocodes.  
21  
22  
23  
24  
25  
26  
27  
28  
29  
30

31  
32 The basic objective of this study is to assess the thermal behavior of composite slabs through  
33 both simple and advanced calculation models and compare their results. More specifically, the  
34 results of the thermo-mechanical analysis, in terms of fire resistance, are compared with the  
35 expected fire resistance that results following the provisions of Eurocode 4, Part 1-2 [13].  
36  
37 Despite the significantly simplified procedure proposed by this norm, its application in the case  
38 of continuous composite slabs requires the involvement of a nonlinear iterative procedure. The  
39 comparison is performed mainly in order to evaluate the effectiveness of simplified methods that  
40 are based on the proposals of Eurocode 4. Moreover, the results of the thermal analysis which is  
41 conducted according to the principles of the heat transfer theory, applied through the finite  
42 element method, are compared with the temperature profiles for composite slabs proposed by  
43 Eurocode 4 [13].  
44  
45  
46  
47  
48  
49  
50  
51  
52

53  
54 Another objective of the paper is to study the fire performance of the steel-concrete slabs  
55 considering two structural systems: a simply supported and a two span continuous one. The two  
56 systems are designed to have the same load bearing capacity at room temperature. Therefore, the  
57  
58  
59  
60  
61  
62  
63  
64  
65

1  
2  
3  
4 goal here is to evaluate the effect of static indeterminacy on the fire resistance of composite  
5  
6 slabs.

7  
8 The paper is organized as follows. The 2<sup>nd</sup> Section presents the fundamentals of the heat transfer  
9  
10 theory, on which the coupled numerical analysis is based. The 3<sup>rd</sup> Section presents the considered  
11  
12 problem and its design for room temperature. The 4<sup>th</sup> Section presents procedures for  
13  
14 determining the fire resistance using simplified methods and following the provisions of  
15  
16 Eurocode. The 5<sup>th</sup> Section presents in detail the advanced numerical method, while the 6<sup>th</sup>  
17  
18 Section presents the obtained results, which are compared against those obtained through the  
19  
20 simplified methods of Section 5. Finally, in the Appendix, the proposed numerical procedure is  
21  
22 applied for the simulation of an experimental test included in [14]. The comparison between  
23  
24 numerical and experimental results shows a good agreement, validating therefore the proposed  
25  
26 numerical methodology.

## 27 28 29 **2. Elements of heat transfer theory**

30  
31  
32 The fundamentals of the heat transfer problem that is treated in this study are first briefly  
33  
34 presented. The description is limited only to slabs made with corrugated steel sheeting and  
35  
36 concrete and, in particular, to the case that the slab is exposed to fire beneath it.

### 37 38 39 40 **2.1. Mechanisms of heat transfer**

41  
42  
43 The three basic mechanisms of heat transfer that appear in the specific problem examined here  
44  
45 are the following:

#### 46 47 48 *Convection*

49  
50  
51 Convection is the heat transfer at the interface between a fluid and a solid element. In the case  
52  
53 considered here a specific case appears, termed as free or natural convection, in which the heat is  
54  
55 transferred by the circulation of fluids (in this case the hot air) due to buoyancy from the density  
56  
57 changes induced by the heating itself. Heat transfer through convection takes place only when  
58  
59 the fluid (hot air) comes in contact with the steel sheeting of the composite slab.

## Radiation

Thermal radiation is the exchange of energy through electromagnetic waves that are emitted from a surface or an object (from the fire to the composite slab in this specific case study). The thermal radiation takes place when the temperature of the materials feeding the fire increases, regardless if they come in contact with the slab. As in the case of light, these electromagnetic waves can be absorbed, transmitted or reflected on the corrugated steel sheeting. Therefore, radiation depends on the orientation of the steel sheeting, its specific shape and on its ability to absorb, transmit and reflect the thermal energy.

## Heat conduction

Since the temperature on the slab volume increases or decreases over time, transient state heat transfer takes place in this case study. The transient state heat conduction partial differential equation is written in the form:

$$k_x \frac{\partial^2 T}{\partial x^2} + k_y \frac{\partial^2 T}{\partial y^2} + k_z \frac{\partial^2 T}{\partial z^2} = \rho C \frac{\partial T}{\partial t}, \quad (1)$$

where  $k_x, k_y, k_z$  are the thermal conductivity coefficients of the material in each one of the three spatial directions,  $\rho$  is the density of the material and  $C$  is its specific heat. All the aforementioned quantities depend on the temperature of the material. Moreover, in the case of porous materials, as e.g. the concrete, the specific heat is affected by the evaporation phenomena that occur over a range of temperatures.

## 2.2. Boundary conditions

Boundary conditions should be applied in order to find a solution to equation (1). According to the nature of the specific problem treated here, these boundary conditions are:

- Adiabatic boundary conditions

Adiabatic boundaries can be treated as a special case of the general fixed flux boundary conditions. No heat exchange takes place across such a boundary and the adiabatic boundary condition is written in the form:

$$-k_n \frac{\partial T}{\partial n} = 0. \quad (2)$$

Adiabatic boundaries are used in order to simulate symmetry conditions (no heat exchange takes place along the symmetry axis or surface) or boundaries which are almost completely insulated.

- Boundary conditions at solid-fluid boundaries

In the case that solid boundaries (steel sheeting or concrete surfaces) are in contact with moving fluids (hot or ambient temperature air), the following boundary condition can be written:

$$-k_n \frac{\partial T}{\partial n} = h(T_s - T_\infty) = h\Delta T, \quad (3)$$

where  $h$  is the total heat transfer coefficient and  $\Delta T$  is the temperature difference between the fluid and the solid boundary surface. In this case  $T_\infty$  is the air temperature (assumed as known) and  $T_s$  is the temperature of the solid surface, which is not a priori known, but is calculated as a result of the solution process. For cases which are of interest in structural analysis problems, both convective and radiation heat exchange takes place and (3) can be written in the form

$$-k_n \frac{\partial T}{\partial n} = h_c(T_s - T_\infty) + \Phi \varepsilon_r \sigma (T_s^4 - T_\infty^4), \quad (4)$$

where  $\Phi$  is the configuration or view factor,  $\varepsilon_r$  is the resultant emissivity (which depends on the fluid and solid emissivities),  $\sigma$  is the Stefan-Boltzmann constant and  $h_c$  is the convective heat transfer coefficient. The first part of the r.h.s. of Eq.(4) is known as the convective term whereas the second one is known as the radiative term. The term  $\varepsilon_r$  can be evaluated by the simple formula

$$\varepsilon_r = \varepsilon_f \times \varepsilon_s, \quad (5)$$

where  $\varepsilon_f$  is the emissivity of fire (usually taken equal to 1.0) and  $\varepsilon_s$  is the emissivity of the structural material.

The calculation of the convective heat transfer coefficient  $h_c$  depends on the type of the convection that takes place (forced convection or natural convection) and is related to the fluid

properties, the orientation of the surface and the type of flow (laminar or turbulent). For the case of the fire-solid boundary conditions, where the natural convection takes place, the flow is turbulent and the  $h_c$  can be calculated according to the following equation [15]:

$$h_c = 0,14 \left[ \left( \frac{g \times P_r}{T \times \nu^2} \right) \right]^m k (\Delta T)^m = \alpha (\Delta T)^m, \quad (6)$$

Here  $\Delta T$  is the temperature difference between the fluid and the solid surface,  $P_r$  is the Prandtl number,  $T$  is the absolute temperature of the air,  $\nu$  is the relative viscosity of the fluid,  $k$  is the thermal conductivity of the air and  $m$  is a coefficient that depends on the side of the structural elements (fire side or ambient temperature air side). Using the appropriate values for  $P_r, T, \nu, k$  for different temperatures and  $g = 9.81 \text{ m/sec}^2$ , the value of  $\alpha$  can be easily calculated.

For further simplification, Eurocode 1 [12] suggests a constant value for the convective heat transfer coefficient  $h_c$ , which depends only on the side of the structural elements (fire side or ambient temperature air side).

### 3. Description of the problem – Design at room temperature

As explained in Section 1, the aim of this study is to evaluate the fire performance of composite slabs through both simple and advanced methods. Two structural systems are considered (see Fig. 1): a simply supported composite slab having a span equal to 3.5 m and a continuous composite slab 7 m long, which consists of two equal spans. The dead load of the slabs is  $G = 3.97 \text{ kN/m}^2$ , while the live load is taken equal to  $Q = 5 \text{ kN/m}^2$ . In both cases the composite slabs are constructed by a trapezoidal steel profile and concrete and they have the same cross-section properties. However, different reinforcement is used, so that the two systems have the same strength at room temperature. The slab has an overall depth of 150 mm. The steel decking is a thin-walled, cold formed profile, made of structural steel FeE320G. It has a depth of 73 mm and a thickness of 1 mm. A normal-weight concrete with calcareous aggregates is used to form the composite slab, which has a compressive strength of 25 MPa and a tensile strength of 2.9 MPa at room temperature. The steel reinforcement has a yield stress equal to 500 MPa.

1  
2  
3  
4  
5  
6 The design of the slabs at room temperature for the ultimate limit state combination  
7  
8 (1.35G+1.5Q) is performed, considering the fact that the load bearing capacity should be the  
9  
10 same for both structural systems. The lower reinforcement of the simply supported slab is first  
11  
12 determined, assuming a single Ø8 bar at every rib of the composite slab (i.e. Ø8/187.5 mm). This  
13  
14 reinforcement is assumed to extend along the total length of the slab for both structural systems.  
15  
16 Then, the upper reinforcement of the continuous slab is calculated, so that it leads to hogging  
17  
18 moment resistance,  $M_{Rd}^-$ , equal to the sagging one,  $M_{Rd}^+$ . The calculations give an upper  
19  
20 reinforcement demand of Ø12/120 mm. This demand is covered by two groups of reinforcement  
21  
22 bars. In the first group, the bars are placed every 240 mm (Ø12/240) and extend along the total  
23  
24 length of the continuous slab. In the second group, the bars are placed every 240 mm (Ø12/240)  
25  
26 and extend from the mid-length of the left span to the mid-length of the right one. This  
27  
28 configuration sums to Ø12/120 over the area of the central support, while the regions near the  
29  
30 left and right outer supports remain with Ø12/240. All the reinforcement bars are assumed to  
31  
32 have a concrete cover of 30 mm. Table 1 summarizes the structural design at room temperature,  
33  
34 for both cases. The design values of the material properties are calculated using the partial safety  
35  
36 factors for fire conditions ( $\gamma_{M,fi} = 1.0$ ).

37  
38 With the application of the above design procedure, the two types of slabs have almost the same  
39  
40 load bearing capacity at room temperature (the small difference comes from the rounding of the  
41  
42 distance between the reinforcements to engineering realistic values). The strength utilization  
43  
44 factor  $\lambda$ , which demonstrates the ratio between the design moment to the resistance moment, is  
45  
46 almost the same for the two considered slab types and is presented in Table 1.

47  
48 The fire design is based on the loading combination for accidental design situations given in  
49  
50 Eurocode 1 [12] and it can be simplified to  $q = G + \psi_{1,1}Q$  (Fig. 1). The combination factor  $\psi_{1,1}$  is  
51  
52 considered here equal to 0.5 according to the Eurocode 0 [16]. This value corresponds to the  
53  
54 building categories A and B, i.e. domestic areas or offices.



## 4. Calculation of the fire resistance through simplified models

In this section the fire resistances in the time and strength domains are calculated for both the examined structural systems, using simplified methods. According to Eurocode 4, Part 1-2 [13], the composite slab satisfies the criterion  $R_x$  when the load-bearing capacity is maintained for the required  $x$  time of fire exposure ( $x$  is expressed in minutes). In this study, the critical time  $t_f$  is calculated, in which the design bending moments for the fire situation reach the corresponding resistances of the structural members. This indicates that the load-bearing capacity is maintained for  $t_f$  minutes (the fire resistance is  $R_{t_f}$ ). During this time period the large deformations are acceptable [17]. For the fire, the ISO 834 standard is adopted [13] that prescribes the evolution of the fire temperature over time.

The mechanical properties of concrete and steel that are used in the calculations are taken according to Eurocode 2, Part 1-2 [18] and Eurocode 3, Part 1-2, [19] respectively. It has to be noticed that both the simplified and the advanced calculation models take into account the fact that the yield strength of steel, the compressive strength of concrete and the modulus of elasticity of both materials are temperature dependent.

The determination of the moment resistances in the case of the simplified models is based on the temperature distribution adopted by Eurocode 4 [13]. The calculations here follow the guidelines of [13, Annex D, (Eq. D.2.1)] and result to the diagrams of Fig. 2 that depict the calculated temperatures for the upper and lower surfaces of the slab, as a function of the fire time. For convenience, the assumed fire temperatures (ISO curve) are also included in this diagram. Here, it should be noticed that Eurocode 4 [13] gives a procedure for the calculation of the temperatures that is valid only till the 120<sup>th</sup> minute of fire. However, in order to be able to continue the calculation of the moment resistance beyond this specific point, the results of the heat transfer analysis (Section 5.4.1) are used. This fact explains the “jump” that occurs in the 120<sup>th</sup> minute in the curve that corresponds to the temperatures of the lower flange of the steel sheeting in Fig. 2. The results of the heat transfer analysis are used also for the calculation of the temperatures of the lower reinforcement the web and the upper flange of the steel sheeting.

1  
2  
3  
4  
5  
6 The determination of the sagging moment resistance  $M_{fi,Rd}^+$  follows equations (4.2) and (4.3) of  
7 [13] that are based on the plastic theory (Fig. 3a). At the  $t$ -th minute of fire exposure, the  
8 temperatures of the various components of the cross-section are assumed to have piecewise  
9 uniform values. In this figure,  $F_C^-$  is the compressive force of the concrete,  $F_{S,rein}^+$  is the tensile  
10 force of the lower reinforcement and  $F_{s,u.f.}^+$ ,  $F_{s,web}^+$ ,  $F_{s,l.f.}^+$  are the tensile forces of the upper flange,  
11 the web and the lower flange of the steel sheeting respectively. Then, the position of the plastic  
12 neutral axis is calculated, on the basis of the equilibrium of the internal forces. Finally, the  
13 moment resistance is calculated by the multiplication of each force with the respective lever arm.  
14 The determination of the hogging resistance moment  $M_{fi,Rd}^-$  follows similar principals (Fig. 3b).  
15 The compressive forces  $F_{s,u.f.}^-$ ,  $F_{s,web}^-$ ,  $F_{s,l.f.}^-$  of the upper flange, the web and lower flange of the  
16 steel sheeting can be easily calculated, given the temperatures of the corresponding parts. The  
17 tensile force of the upper reinforcement,  $F_{S,rein}^+$ , is calculated based on the assumption that it is at  
18 room temperature. The calculation of the compressive force of concrete is more complex and is  
19 based on the method proposed in [13, Annex D, D.3 (7)]. Briefly, an equivalent cross section is  
20 defined with a depth equal to  $h_{eff}$ , which is divided into  $n$  horizontal zones. For each of them  
21 the temperature can be calculated, and therefore it is possible to calculate the corresponding  
22 forces  $F_{C,Ti}^-$ ,  $i = 1, \dots, n$ . Finally, the plastic neutral axis and the corresponding moment resistance  
23  $M_{fi,Rd}^-$  can be easily calculated.  
24  
25  
26  
27  
28  
29  
30  
31  
32  
33  
34  
35  
36  
37  
38  
39  
40  
41  
42  
43  
44  
45

46 The moment resistances are calculated for the basic module of the slab, which is repeated every  
47 187.5mm (see Fig. 1). However for convenience, an equivalent width of 1m is considered,  
48 therefore in the diagrams of Fig. 3 and in the subsequent ones, the moments are given in kNm/m.  
49  
50  
51

## 52 **4.2. Simply supported slab**

53  
54 Taking into account the data given above, it is easily verified that at the 77<sup>th</sup> minute the design  
55 moment resistance  $M_{fi,Rd}$  becomes equal to the design moment  $M_{fi,Sd}$ . Therefore the fire  
56 resistance time for the simply supported system is 77 minutes ( R77). Figure 4 presents the  
57  
58  
59  
60  
61  
62  
63  
64  
65

1  
2  
3  
4 decrease of the moment resistance  $M_{fi,Rd}$  of the simply supported slab with time. The dashed line  
5  
6 in the figure represents the design moment  $M_{fi,Sd}$  .  
7  
8  
9

### 10 **4.3. Continuous slab**

11  
12 The case of the continuous slab is more complex, due to the fact that the system is statically  
13 indeterminate. In this case, the temperature gradient across the depth of the composite slab  
14 creates curvature that cannot be developed freely, producing bending moments. Therefore, in  
15 order to calculate the total bending moments that develop along the  $x$  - axis of the slab, we have  
16 to sum up the bending moments due to the external loading,  $M_q$ , and the bending moments due  
17 to thermal loading,  $M_T$ , i.e.:

$$22 \quad M_{fi,tot}(x) = M_q(x) + M_T(x) \quad (7)$$

23  
24  
25  
26  
27 Of course, the above equation holds as long as the developed moments are smaller than the  
28 corresponding resistances. In order to calculate  $M_T$ , it is assumed that the temperature variation  
29 across the depth of the slab is linear. The temperature difference is calculated from the curves of  
30 Fig. 2. Due to the fact that the slab is statically indeterminate, the magnitude of the moments  $M_T$   
31 depends on the bending rigidity  $EJ$  (where  $E$  denotes the modulus of elasticity and  $J$  the  
32 second moment of inertia of the cross section of the slab). On the other hand,  $J$  depends on the  
33 value of the developed total bending moment  $M_{fi,tot}$ , due to the nonlinear behavior of the  
34 concrete in tension. Moreover, as the properties of the materials change with temperature, the  
35 bending rigidity changes as well. For the above reasons, the calculation of the moment diagram  
36  $M_{fi,tot}(x)$  can be obtained only through an iterative process. First,  $(EJ - M)$  diagrams were  
37 created for characteristic instants of the fire loading (see Fig. 5a and 5b) and the length of the  
38 continuous slab was discretized into 20 equal frame finite elements. The basic steps of the  
39 iterative calculation procedure are given in the sequel. For convenience, the various quantities  
40 are equipped with a upper left index denoting the temperature for which the respective quantity  
41 occurs, i.e.  ${}^T M$  denotes the bending moment for the temperature  $T$ . The procedure is also  
42 demonstrated graphically in Fig. 6.  
43  
44  
45  
46  
47  
48  
49  
50  
51  
52  
53  
54  
55  
56  
57  
58  
59  
60  
61  
62  
63  
64  
65

1  
2  
3  
4 **Step 1: Initializations**

- 5  
6 • Set temperature to room conditions ( $T = 20^\circ C$ ).  
7  
8 • Select temperature step  $\Delta T$  (e.g.  $\Delta T = 5^\circ C$ ).  
9  
10 • Select the accuracy of the iterative procedure  $\varepsilon$  (i.e.  $\varepsilon$  is a small number).  
11  
12

13  
14 **Step 2:** Calculate the moment distribution  $M_q(x)$  due to the fire design load  $q = G + \psi_{1,1}Q$ .  
15

16 **Step 3:** Increase temperature by  $\Delta T$  and calculate the new temperature  $T$  and the temperatures  
17 of the upper and lower slab surface (Fig. 3).  
18  
19

20 **Step 4:**

21 **Step 4a**

- 22  
23 • Set  $i = 1$ .  
24  
25 • Set as an initial approximation for the moments of the current temperature  $T$ , the ones  
26 from the previous temperature step, i.e.  ${}^T M_{fi,tot}^{(1)}(x) = {}^{T-\Delta T} M_{fi,tot}(x)$ .  
27  
28  
29

30 **Step 4b**

- 31  
32 • Calculate the updated rigidities  ${}^T EJ^{(i)}$  using the appropriate  $(EJ - M)$  curve for the  
33 temperature  $T$ .  
34  
35 • Calculate the moment diagram  ${}^T M_T^{(i)}(x)$  according to the reduced rigidities  ${}^T EJ^{(i)}$  of the  
36 finite element of the slab.  
37  
38 • Calculate the total moment diagram  ${}^T M_{fi,tot}^{(i)}(x)$  through equation (7).  
39  
40 • If  $\left| {}^T M_{fi,tot}^{(i)} - {}^T M_{fi,tot}^{(i-1)} \right| \leq \varepsilon$ , then the new moment values differ very little from the previous  
41 ones, therefore convergence has been attained for temperature  $T$ , i.e.  
42  
43  
44

45  
46  ${}^T M_{fi,tot}(x) = {}^T M_{fi,tot}^{(i)}(x)$ . In this case go to Step 5. Else, set  $i = i + 1$  and repeat Step 4b.  
47  
48

49 **Step 5:** Compare the moment developed at the support B,  ${}^T M_{B,fi,tot}$ , with the corresponding  
50 resistance  ${}^T M_{B,fi,Rd}^-$ . If  ${}^T M_{B,fi,tot} < {}^T M_{B,fi,Rd}^-$ , then continue with Step 3. If  ${}^T M_{B,fi,tot} = {}^T M_{B,fi,Rd}^-$ ,  
51 then the strength at the support has been exhausted and a plastic hinge is formed at this point.  
52 Therefore, from this point on, the slab can be considered as statically determinate and the  
53 calculations are simplified because the temperature gradient has no additional effect on the  
54 bending moments that develop.  
55  
56  
57  
58  
59  
60  
61  
62  
63  
64  
65

1  
2  
3  
4 **Step 6:** Now, the moment diagrams for the following temperature increments can be easily  
5 calculated. For each temperature increment, the new moment resistance for point B is calculated  
6  
7  ${}^T M_{B,fi,Rd}^-$ . The moment diagram is constructed setting the moment at the support equal to the  
8  
9 resistance moment and redistributing the moments at the spans so that equilibrium is satisfied. If  
10 the maximum moment appearing at the span  $M_{sp,fi,tot}$ , has reached the sagging resistance moment  
11  
12  ${}^T M_{fi,Rd}^+$ , then the slab has reached its ultimate load resistance and the fire resistance time has  
13  
14 been determined.  
15  
16  
17  
18  
19

20 The above procedure was applied with a temperature step  $\Delta T = 5^\circ C$ . After parametric studies, it  
21 was concluded that this value provided a good balance between accuracy and efficiency. With  
22 the results of this procedure, the diagram of Fig. 7 is constructed which gives the resistance  
23 moments  $M_{fi,Rd}^+$ ,  $M_{fi,Rd}^-$  and the design moments  $M_{B,fi,tot}$  and  $M_{sp,fi,tot}$  for the internal support and  
24 for the spans, respectively, as a function of the fire time. The moment at the support reaches the  
25 resistance moment at the 15th minute of the ISO fire (Fig. 7). After this point, moment  
26 redistribution takes place. Since the system becomes statically determinate, the temperature  
27 gradient at the cross section of the slab produces thermal bowing only and not additional  
28 moments. As the fire continues, the moment increases at the span while both the hogging and  
29 sagging resistance moments decrease. At a critical time, both the sagging moment and the  
30 hogging moment reach to the corresponding resistance values and the slab becomes  
31 kinematically unstable. This happens at the 170th minute of the ISO fire, i.e the continuous slab  
32 has a fire resistance of R170. The procedure and the corresponding moment diagrams are  
33 illustrated in Fig. 8.  
34  
35  
36  
37  
38  
39  
40  
41  
42  
43  
44  
45

46 It must be noticed that the fire resistance of the continuous slab is much higher than the fire  
47 resistance of the simply supported slab, despite the fact that they have the same load bearing  
48 capacities at room temperature. Moreover, this conclusion holds despite the unfavorable (at a  
49 first glance) effect of the thermal gradient in the case of the continuous slab. Actually, the  
50 temperature difference between the upper and the lower side of the composite slab is remarkable  
51 even from the first minutes of the fire exposure (at the 15<sup>th</sup> minute the temperature difference is  
52 about 300° C) and this demonstrates that the thermal gradient effect is important in the case of  
53 the continuous slab. The influence of the bending moments due to the thermal gradient is  
54  
55  
56  
57  
58  
59  
60  
61  
62  
63  
64  
65

1  
2  
3  
4 different for the internal support and for the span. At the internal support the design moment  
5 reaches quickly the resistance moment because the negative moment due to the external loading  
6 is enlarged by the negative moment due to the thermal gradient. After the first plastic hinge is  
7 formed, moment redistribution takes place and the moment at the support remains equal to the  
8 resistance moment, which is, however, modified with time. At the span the moment due to the  
9 design load is positive and the addition of the negative moment due to the thermal gradient leads  
10 to a reduction of the total value of bending moment. The reduction is considerable and for this  
11 reason the collapse is prevented until the 170<sup>th</sup> minute.  
12  
13  
14  
15  
16  
17  
18  
19

## 20 **5. The advanced calculation model**

### 21 **5.1. Development of the numerical model**

22  
23 The numerical analysis was carried out using the nonlinear finite element code MSC-MARC  
24 [20]. Due to the fact that composite slabs are formed using continuous profiled sheeting, it is  
25 adequate to simulate a section which is 187.5 mm wide (Fig. 9). Moreover, due to the symmetry  
26 of this section with respect to the vertical axis, it is adequate to finally model only half of this.  
27 For further simplification, as trying to reduce the computational cost which is associated with the  
28 nonlinear three-dimensional modeling, only half of the total length of the slab is considered,  
29 using the appropriate symmetry boundary conditions. These simplifications will not affect the  
30 results, which will be identical with those of the full model. Therefore, for the simply supported  
31 slab, a length equal to 1.75 m is modelled using the following boundary conditions (Fig. 10a):  
32  
33  
34  
35  
36  
37  
38  
39  
40  
41

- 42 • Fixed displacement  $d_y = 0$  and fixed rotation  $R_x = 0$  for all the nodes on the  $x - z$  symmetry  
43 plane.  
44
- 45 • Fixed displacement  $d_x = 0$  and fixed rotation  $R_y = 0$  for all the nodes on the  $y - z$   
46 symmetry plane.  
47
- 48 • Fixed displacement  $d_z = 0$  for the lower edge nodes of the end of the slab corresponding to  
49 the roller support.  
50

51 For the case of the continuous slab the half of the total length is modeled which is equal to 3.5m.  
52

53 The boundary conditions that are used are the following (Fig. 10b):  
54  
55  
56  
57  
58  
59  
60  
61  
62  
63  
64  
65

- Fixed displacement  $d_y = 0$  and fixed rotation  $R_x = 0$  for all the nodes on the  $x - z$  symmetry plane
- Fixed displacements  $d_x = 0$  and  $d_z = 0$  and fixed rotation  $R_y = 0$  for all the nodes on the  $y - z$  symmetry plane that coincides with the position of the internal support.
- Fixed displacement  $d_z = 0$  for the lower edge nodes of the end of the slab corresponding to the roller support.

The models developed for the simulation of the composite slabs utilize three different types of elements. The steel profile was modeled through four-node shell elements while concrete was simulated with three-dimensional solid elements. The nodes of the shell elements were connected to the corresponding nodes of the 3D-solid elements of concrete (Fig. 11). Two-node, 3D frame elements were used for modeling the reinforcing bars. The numbers of the finite elements used for the representation of the simply supported slab and for the continuous slab are given in Table 2.

The thermal properties of the materials (thermal conductivity and specific heat) are assumed to be temperature dependent as it is defined in [18], [19] for concrete and steel respectively.

Moreover, the yield strength of steel, the compressive and tensile strength of concrete and the modulus of elasticity of both materials are temperature dependent.

It should be noted that the advanced numerical model assumes a perfect bond between the steel sheeting and the concrete. Concerning the possible debonding that has been observed during fire tests (e.g. [14] and [21]), it is recalled that the phenomenon is local and it has been observed in composite slabs with steel sheeting of considerable height [14]. Moreover, according to the experimental results that are presented in [14] and [22], the typical failure mode for fire exposed composite slabs is flexural. The longitudinal shear failure that is observed at room temperature does not usually arise in fire tests. This can be attributed to the fact that the temperature of the steel decking increases rapidly during the fire, its strength is significantly reduced and the tensile forces are undertaken by the reinforcing bars. Therefore, longitudinal shear failure does not seem to be a critical phenomenon during fire exposure and flexural failure is expected. The above remarks fully justify the assumption of the complete bonding between the steel sheeting and the concrete, which has also been adopted by several former numerical studies on the same subject (see e.g. [5], [14], [23]).

## 5.2. Thermal boundary conditions

The following thermal boundary conditions were taken into account (Fig. 12).

- Along the symmetry boundaries, adiabatic boundary conditions were considered.
- On the upper side of the composite slab (ambient air side), a solid-fluid boundary condition was considered. In Eq. (4) the convective heat transfer coefficient was assumed to be constant and equal to  $h_c = 4 \text{ W/m}^2\text{K}$ . Moreover, according to Eurocode 1 [12], the second term of the r.h.s of Eq. (4) was ignored.
- On the lower side of the composite slab (fire side), solid-fluid boundary conditions were also considered. According to [12], the convective heat transfer coefficient was assumed to be constant and equal to  $h_c = 25 \text{ W/m}^2\text{K}$ . In the second term of the r.h.s of Eq. (8) the emissivity of fire  $\varepsilon_f$  and the emissivity of the construction material  $\varepsilon_m$  (in this case the corrugated steel sheeting) were considered according to [12]. The parameters were taken as  $\varepsilon_f = 1.0$  and  $\varepsilon_m = 0.7$  respectively. The view factor of the lower flange of the profiled steel sheeting was taken equal to  $\Phi_{l.f.} = 1.0$ . The view factors for the web and for the upper flange of the steel sheeting were calculated following the approach first developed in [24] and adopted also by Eurocode 4, Part 1-2 [13]. The calculations for the specific profile used here gave  $\Phi_{web} = 0.510$  and  $\Phi_{u.f.} = 0.647$  for the web and the upper flange respectively.

Additionally, parametric analyses were conducted in order to investigate if the simplification adopted by Eurocode 1 [12] about the constant value of the convective heat transfer coefficient  $h_c$ , affects the heat transfer analysis and, consequently, the mechanical analysis that follows. In the latter, the parameters of Eq. (6) were taken according to [15], as  $\alpha = 2.2$  and  $m = 1/4$  for the upper side of the slab (air side) and  $\alpha = 1.0$  and  $m = 1/3$  for the lower side of the slab (fire side). In the first analysis series the convective heat transfer coefficient was considered as constant, while in the second analysis series a variable heat transfer coefficient was used.



### 5.3. Analysis

The numerical analysis for the determination of the fire resistance of the composite slab is a demanding task because various non-linear phenomena evolve during the fire exposure:

- Non-linear material response for both steel and concrete, including the possible cracking of concrete due to its low tensile strength.
- Dependence of all the mechanical and thermal properties of the materials on temperature.
- Convective and radiation heat exchange on the boundaries of the composite slab (lower and upper surfaces). Consequently, a non-linear temperature distribution across the section of the slab arises.

In the present paper, the behavior of the composite slab in elevated temperatures is modeled through combined thermal-mechanical analysis which takes into account all the aforementioned non-linear effects. The temperature increase contributes to the deformation of the slab through thermal strains and also influences the properties of the materials. Actually, a heat transfer analysis is first performed which is followed by a stress analysis.

In this case study the composite slabs are exposed to the standard ISO 834 fire curve for 240 minutes and the problem is simulated through transient heat transfer under constant imposed load. It is noticed that the loading is applied prior to the increase of the temperature. The temperature distribution is assumed to be constant along the length of the slab. The initial temperature for the composite slab is taken equal to 20° C.

## 6. Results of the numerical analysis

### 6.1. Results of the heat transfer analysis

Figure 13 gives the temperatures at characteristic points of the cross-section of the slab. It is noticed that the maximum temperatures that are obtained for the lower flange are close to the corresponding values of the standard fire curve. The temperature at points F and G is quite lower due to the reduced incident thermal radiation on the web and the on upper flange. In the concrete, as the distance from the steel decking is increasing, the temperature decreases. As expected, the minimum values are calculated for the upper part of the slab. The temperature of the lower flange of the steel decking after the 20<sup>th</sup> minute of the analysis (points A, H) is very high.

1  
2  
3  
4  
5  
6 According to Eurocode 4 [13], the decisive fire resistance time with respect to the maximum  
7 temperature rise, is calculated equal to 70 minutes. For that time the temperature of points E, D  
8 at the upper side of the concrete slab does not exceed the value of 180° C. Therefore, the slab  
9 satisfies the “I” criterion for thermal insulation.

10  
11  
12  
13 The temperature distribution that is illustrated in Fig. 14 depicts accurately the isotherms of the  
14 cross section. The differentiation of the temperature in the horizontal planes is due to the  
15 presence of the ribs. The developed temperature pattern is absolutely similar with the one that is  
16 indicated in [13, Fig. D.3.2.a], however, the temperature values present some differences. Table  
17 3 gives the comparison between the numerically obtained results for the temperatures of the  
18 various parts of the profiled steel sheeting and of the lower steel reinforcement, with respect to  
19 those obtained by applying the procedures of Eurocode 4 [13] for the same problem. It is noticed  
20 that the values of temperature resulting from the heat transfer analysis are greater with respect to  
21 those obtained by applying Eurocode 4. For the steel reinforcement the differences are quite  
22 small. However, significant differences are observed for the temperatures of the steel sheeting. In  
23 this respect, it seems that the procedures of Eurocode 4 are not on the safe side for the type of  
24 corrugated steel sheeting used in this paper.  
25  
26  
27  
28  
29  
30  
31  
32  
33  
34  
35

36 Figs 15 and 16, give the comparison between the results obtained by the two series of heat  
37 transfer analyses (the series adopting the variable convective heat transfer coefficient and the  
38 series adopting the constant one). More specifically, the mean temperatures obtained for the  
39 lower flange (Fig. 15) and for the web (Fig. 16) are compared. In the same figures, the  
40 corresponding values obtained by the application of Eurocode 4 [13] are presented. It is clear that  
41 for both cases the results of the numerical analyses are very close. It has to be noticed that after  
42 the 60<sup>th</sup> minute the results coincide. Thus, it is obvious that the simplification adopted by  
43 Eurocode 4 [13] for the constant value of the convective heat transfer coefficient is reasonable,  
44 as the usage of the more accurate description of  $h_c$  leads to almost the same results. Moreover,  
45 this fact indicates that the solution of the coupled thermo-mechanical problem is not affected by  
46 this parameter.  
47  
48  
49  
50  
51  
52  
53  
54  
55  
56  
57  
58  
59  
60  
61  
62  
63  
64  
65

## 6.2. Results of the mechanical analysis

The curves of Fig. 17 give the evolution of the maximum vertical displacement of the two types of slabs with respect to time. For the case of the simply supported composite slab, the collapse occurs at the 67<sup>th</sup> minute. The response of the continuous composite slab is completely different and it finally collapses at the 226<sup>th</sup> minute. In both cases, just before collapse occurs, significant deformations at the span are observed. The difference in the response was explained in detail in the previous section and lies mainly on the moment redistribution that takes place during the fire exposure in the case of the continuous slab. Also, in this case, the temperature gradient at the cross-section of the slab affects in a positive way the mechanical problem. In both cases, the contribution of the profiled steel sheeting in the resistance of the composite slab is quite limited in elevated temperatures. Moreover, it is noticed that in both cases the values of the maximum vertical deflections of the composite slabs are significantly increased in elevated temperatures. In practice, deflection limits are imposed in order to avoid excessive deformations [25]. For the flexural members the limit value that is usually used is

$$\delta_{\max} = \frac{L^2}{400d}, \quad (8)$$

where  $d$  is the depth of the section and  $L$  is the length of the span. The application of the above criterion for the cases treated here gives  $\delta_{\max} = 204$  mm. This occurs around the 62<sup>nd</sup> minute for the simply supported slab, while the continuous slab reaches the limit deflection approximately at the 152<sup>nd</sup> minute. Another limitation for the flexural structural members that is referred to DIN 4102 [26] is the rate of deflection. This criterion is expressed in the form

$$\frac{du}{dt} \leq \frac{L^2}{9000d}, \quad (9)$$

where  $du$  is the change in deflection (mm) during a time interval  $dt$  of one minute. Fig. 18 presents the calculated deflection rate for the two slab systems. In the cases treated here, the limiting rate of deflection is calculated to be 9.07 mm/min. For the simply supported slab, this limiting rate is reached in the 62<sup>nd</sup> minute, while in the case of the continuous slab this happens approximately at the 203<sup>rd</sup> minute.

1  
2  
3  
4 Figure 19 illustrates the deformed shape of the simply supported slab and the equivalent cracking  
5 strain at the 30<sup>th</sup> and 67<sup>th</sup> minutes of analysis. The development of cracking starts rather early. At  
6 the time of 30 minutes various cracks have already been formed in the composite slab. As the  
7 time increases, the cracking develops towards the upper side of the slab. Significant cracking is  
8 noticed also in the interface between the concrete and the steel reinforcement.

9  
10 For the case of the continuous slab, the deformed shape and the cracking strains are illustrated in  
11 Fig. 20. The left part of the figure corresponds to the internal support of the slab. At the time of  
12 60 minutes various distinct cracks have already developed at the upper part of the slab near the  
13 support. However, even at the time of the 120 minutes, the cracking at the lower part of the slab  
14 is very limited along the span, indicating that the values of the sagging moments are still very  
15 low. The situation is different at the 180 minutes and the significant deformations are obvious.  
16 Significant cracking appears in the vicinity of the support and at the mid-span. This is a sign that  
17 the resistances of the slab are progressively exhausted. The above findings compare well with the  
18 corresponding results of the simplified model, as they are expressed through the diagrams of Fig.  
19 8.

20  
21  
22  
23  
24  
25  
26  
27  
28  
29  
30  
31  
32  
33 Finally, it is interesting to compare the results, in terms of obtained fire resistance between the  
34 simplified and the advanced models. It has to be noticed first that a direct comparison between  
35 them is not possible, because the fire resistance in the simplified models is defined through the  
36 attainment of the ultimate strength of the structural systems while in the case of the advanced  
37 models the fire resistance is defined through maximum deflections or deflection rates. However,  
38 some qualitative comparison is still possible.

39  
40  
41  
42  
43  
44  
45  
46 In section 4.1, the simply supported slab was found to have, according to Eurocode 4 [13], a load  
47 bearing capacity for 77 minutes. On the other hand, the collapse of the corresponding numerical  
48 model (as it is indicated in Fig. 17) occurred in the 67<sup>th</sup> minute. It can be easily verified by  
49 studying all the displayed results that the main reason for this difference is the fact that the  
50 temperature values calculated for the steel sheeting following Eurocode 4 [13] are lower  
51 compared with the respective values that result from the thermal analysis. Therefore, the sagging  
52 moment resistance is greater in the case of the simplified model.

1  
2  
3  
4 The resistance of the continuous slab seems to be dominated by the effects of the temperature  
5 gradient and by the stress redistribution that takes place when the resistance at the position of the  
6 internal support is exhausted. In section 4.2, the continuous slab was found to have, according to  
7 Eurocode 4 [13], fire resistance for 170 minutes. On the other hand, the numerical analysis  
8 indicated that the failure occurs at the 226<sup>th</sup> minute. At a first glance this difference seems  
9 striking, however, it should be examined having in mind all the simplified assumptions included  
10 in the simplified model. More specifically, in the simplified model the ultimate state was  
11 achieved when the moment resistance at mid-span became equal to the design moment (at the  
12 170<sup>th</sup> minute) leading to an unstable system, while in the numerical model the failure was  
13 indicated by the inability of the solution procedure to converge to a solution due to large strain  
14 increments. Of course, the above two failure criteria are not directly comparable. One more  
15 reason making comparisons very delicate in this situation, is the fact that the ISO curve  
16 temperature at the 170<sup>th</sup> minute is 1101 °C, while at the 226<sup>th</sup> minute it is 1144 °C, i.e. the  
17 temperature differences become very small as the time increases, making the accurate estimation  
18 of the failure state in terms of strength a very delicate issue. Except the above, it should be  
19 reminded here that the calculation of moment resistances in the case of the simplified models  
20 was based upon certain simplifications introduced by Eurocode 4 with respect to the calculation  
21 of the temperatures of the components of the composite slab. Following the code, the  
22 temperatures were assumed to be uniform along the horizontal zones of the concrete. Moreover,  
23 each part of the steel sheeting (upper flange, web and lower flange) is supposed to have a  
24 uniform temperature. The above are illustrated in Fig. 3. Obviously, as it results from the plot of  
25 Fig. 14, this assumption is not absolutely correct and may lead to some differences in the  
26 bending moment resistances that are calculated by the two methods. Table 4 summarizes the  
27 obtained fire resistances for both structural systems, in the time domain.  
28  
29  
30  
31  
32  
33  
34  
35  
36  
37  
38  
39  
40  
41  
42  
43  
44  
45  
46  
47

## 48 **7. Conclusions**

49 The paper presents the accurate thermo-mechanical modeling of the behavior of a simply  
50 supported and of a continuous two-span slab, which are submitted in elevated temperatures  
51 according to the standard ISO fire curve. The numerical models are based on combination of  
52 three dimensional finite elements for the concrete, shell elements for the profiled steel sheeting  
53 and frame elements for the steel reinforcement. All the necessary mechanical and thermal  
54  
55  
56  
57  
58  
59  
60  
61  
62  
63  
64  
65

1  
2  
3  
4 boundary conditions are taken into account and symmetry procedures are applied in order to  
5 reduce the dimensions of the numerical problem. In parallel, the same problems are studied  
6 through simplified methods based upon the recommendations of Eurocode 4 for the  
7 determination of the temperatures of the various parts of the composite slab and for the  
8 calculation of the sagging and hogging moment resistances. An algorithm is introduced, that  
9 facilitates the determination of the fire resistance time within this simplified framework.  
10  
11  
12  
13  
14  
15  
16

17 The main conclusions of the study are the following:

- 18 • The continuous slab seems to have a significantly improved behavior in elevated  
19 temperatures with respect to the simply supported one. This result is verified by both the  
20 simple and the advanced solution procedures.  
21  
22
- 23 • The temperatures obtained by means of the advanced thermal analysis are higher compared  
24 to the ones determined by means of the simplified procedures specified in the Eurocodes.  
25 The differences are more significant for the thin-walled steel sheeting and may lead to fire  
26 resistance times which are smaller compared to the ones calculated through Eurocode 4. For  
27 the case of the simply supported slab, if deflection limits are respected, this reduction is of  
28 the order of 5 minutes. For the case of the continuous slab, the definition of fire resistance  
29 time for the advanced model depends strongly on the applied criterion. The strictest criterion  
30 in the case examined here was found to be the one related with the deflection. The fire  
31 resistance time determined according to this criterion is in rather good agreement with the  
32 one calculated through the simplified model which is based on strength (152 minutes and 170  
33 minutes respectively).  
34  
35  
36  
37  
38  
39  
40  
41  
42  
43  
44  
45  
46

## 47 **Appendix: Validation of the numerical model**

48  
49  
50 The validation of the numerical model proposed in this study is based on the experimental results  
51 that are reported by Hamerlinck in [14]. During this experimental program, fire tests were  
52 conducted in order to investigate the behavior of composite slabs during exposure to standard  
53 fire. The verification of the current advanced model is based on test No.2, as it is referred in [14],  
54  
55  
56  
57  
58  
59  
60  
61  
62  
63  
64  
65

1  
2  
3  
4 which is a fire test on a simply supported, one-way composite slab (similar to the one studied in  
5 this paper).  
6  
7

8  
9  
10 The total span of the test specimen is equal to 3.2 m, as it is illustrated in Fig. 21. The test is  
11 performed on a slab with Prins 73 steel sheeting with thickness equal to 1 mm. The self-weight of  
12 the slabs is  $G = 2.7 \text{ kN/m}^2$ , while the imposed load is equal to  $Q = 3 \text{ kN/m}^2$ . The loading was  
13 applied by four point loads (see Fig. 21). The positive reinforcement is equal to  $\text{Ø}10/208$  while  
14 the negative one is  $\text{Ø}6/150$  and they are defined as hot-rolled and cold worked respectively. The  
15 concrete depth which is equal to 173 mm. During the fire test, thermocouples were used for the  
16 measurement of the temperature of the steel sheeting, of the reinforcement and of various points  
17 in concrete. The accurate dimensions of the cross-section and the arrangement of the reinforcing  
18 bars are illustrated in Fig. 22 while the position of the thermocouples is presented in Fig. 23.  
19 The mechanical properties of steel and concrete were measured at room temperature during the  
20 experimental program and they are presented in Table 5.  
21  
22  
23  
24  
25  
26  
27  
28  
29  
30

31  
32 The finite element model that is developed in order to compare the numerical with the  
33 experimental results follows all the principles that were described in Section 5.2. All the  
34 mechanical and thermal material properties are assumed to be temperature dependent according  
35 to [18], [19] for concrete and steel respectively. The material characteristics measured during the  
36 experimental program are taken into account. Moreover, the appropriate distinction is made for  
37 hot-rolled and cold-worked steel.  
38  
39  
40  
41  
42  
43

44 The thermal boundary conditions are considered in the same way as they were presented in  
45 Section 5.2. For the emissivities, the values used in [14] were adopted. Finally, it is noted that the  
46 analysis takes into account all the considerations that were described in Section 5.3.  
47  
48  
49  
50

51 The comparison of the numerical and the experimental results, considering the thermal response,  
52 is illustrated in Fig. 24. In general, a good agreement between the measured and calculated  
53 values is observed.  
54  
55  
56  
57  
58  
59  
60  
61  
62  
63  
64  
65

1  
2  
3  
4 Considering the evaluation of the mechanical response of the slab, it is noted a very good  
5 agreement between the measured and the calculated deflections until the 97<sup>th</sup> minute of the fire  
6 exposure (Fig. 25). After this minute the numerical analysis stops due to numerical problems  
7 attributed to the significant cracking of concrete.  
8  
9

10  
11  
12  
13 In general, it can be concluded that the numerical model represents accurately both the thermal  
14 and the mechanical response of the studied composite slab under fire conditions.  
15  
16  
17

## 18 19 **8. Acknowledgments**

20  
21  
22 This research has been co-financed by the European Union (European Social Fund – ESF) and  
23 Greek national funds through the Operational Program "Education and Lifelong Learning" of the  
24 National Strategic Reference Framework (NSRF) - Research Funding Program: Heracleitus II.  
25 Investing in knowledge society through the European Social Fund.  
26  
27  
28  
29

## 30 31 **References**

- 32  
33  
34 [1] Thomson GC, Moxon K, Preston RR (1987) Contract Report to Steel Construction  
35 Institute. Indicative Fire Test on Composite Concrete/Steel Deck Floor System.  
36  
37 [2] The Steel Construction Institute (2008) Report to Corus CSD. Slimflor Compendium.  
38 Document RT1147 Version 01.  
39  
40 [3] Bailey CG, White DS, Moore DB (2000) The tensile membrane action of unrestrained  
41 composite slabs simulated under fire conditions, Eng. Struct. 22:1583-1595.  
42  
43 [4] Hamerlinck AF, Twilt L, Brekelmans JWPM, Van de Haar PW (1990) The mechanical  
44 behaviour of fire-exposed composite steel/concrete slabs under negative bending. Test  
45 report, Research Report BI-90-118, Eindhoven University of Technology/TNO-Building  
46 and Construction Research.  
47  
48 [5] Gille M, Usmani A, Rotter M, O' Connor M (2001) Modeling of heated composite floor  
49 slabs with reference to the Cardington experiments, Fire Safety J. 36: 745-767.  
50  
51 [6] Huang Z, Burgess I, Plank R (2000) Effective stiffness modeling of composite concrete  
52 slabs in fire, Eng. Struct. 22: 1133-1144.  
53  
54 [7] Vulcan (2008) Vulcan Solutions Ltd, <http://www.vulcan-solutions.com/index.html>  
55  
56  
57  
58  
59  
60  
61  
62  
63  
64  
65



- 1  
2  
3  
4 [8] Yu X, Huang Z, Burgess I, Plank R (2008) Nonlinear analysis of orthotropic slabs in fire,  
5 Eng. Struct. 30: 67-80.  
6  
7  
8 [9] Gillie M, Usmani AS, Rotter JM (2001) A structural analysis of the first Cardington test, J.  
9 Constr. Steel Res. 57: 581-601.  
10  
11 [10] Lamont S, Usmani AS, Drysdale DD (2001) Heat transfer analysis of the composite slab in  
12 the Cardington frame fire tests, Fire Safety J. 36: 815-839.  
13  
14  
15 [11] Cashell KA, Elghazouli AY, Izzuddin BA (2011) Failure Assessment of Lightly  
16 Reinforced Floor Slabs. II: Analytical Studies, J struct eng-ASCE. 137: pp 989-1001.  
17  
18 [12] European Committee for Standardization (2002) Eurocode 1. EN 1991-1-2. General  
19 actions-Actions on structures exposed to fire – Part 1-2. General actions-Actions on  
20 structures exposed to fire.  
21  
22  
23  
24 [13] European Committee for Standardization (2003) Eurocode4. EN 1994-1-2. Design of  
25 composite steel and concrete structures. Part 1-2. General rules – Structural fire design.  
26  
27 [14] Hamerlinck AF(1991) The behaviour of fire exposed composite steel/concrete slabs, PhD  
28 thesis, Eindhoven University of Technology.  
29  
30 [15] Wang YC (2002) Steel and composite structures: behavior and design for fire safety, first  
31 ed., Spon Press, London.  
32  
33  
34  
35 [16] European Committee for Standardization (2002) Eurocode 0. EN 1990. Basis of structural  
36 design.  
37  
38  
39 [17] Franssen JM, Vila Real P (2010) Fire Design of Steel Structures, first ed., Ernst & Sohn,  
40 Berlin.  
41  
42 [18] European Committee for Standardization (2002) Eurocode 2. EN 1992-1-2. Design of  
43 concrete structures – Part 1-2. General rules – structural fire design.  
44  
45 [19] European Committee for Standardization (2003) Eurocode 3. EN 1993-1-2. Design of steel  
46 structures – Part 1-2. General rules – structural fire design.  
47  
48  
49 [20] MSC Software Corporation (2010) MSC Marc, Volume A: Theory and User Information,  
50 Version.  
51  
52  
53 [21] Newman GM, Robinson JT, Bailey CG (2000) Fire safe design: a new approach to multi-  
54 story steel-framed buildings, Berkshire (UK): The Steel Construction Institute.  
55  
56 [22] Both C (1998), The fire resistance of composite steel-concrete slabs, PhD thesis,  
57 Eindhoven University of Technology.  
58  
59  
60  
61  
62  
63  
64  
65

1  
2  
3  
4  
5  
6  
7  
8  
9  
10  
11  
12  
13  
14  
15  
16  
17  
18  
19  
20  
21  
22  
23  
24  
25  
26  
27  
28  
29  
30  
31  
32  
33  
34  
35  
36  
37  
38  
39  
40  
41  
42  
43  
44  
45  
46  
47  
48  
49  
50  
51  
52  
53  
54  
55  
56  
57  
58  
59  
60  
61  
62  
63  
64  
65

[23] Lim L, Buchanan A, Moss P, Franssen JM (2004) Numerical modeling of two way concrete slabs in fire, Eng. Struct. 26:1081-1091.

[24] Wickström U, Sterner E (1990) TASEF, Temperature analysis of structures exposed to fire-user's manual, Swedish National Testing Institute, SP report 05.

[25] Purkiss JA (2007), Fire safety Engineering – Design of structures, second ed., Butterworth – Heinemann, Oxford.

[26] DIN 4102 – Part 2 (1977) Fire behavior of building materials and building components. Building Components Definitions, Requirements and Tests.

1  
2  
3  
4 **FIGURE AND TABLE CAPTIONS**  
5  
6

7 **Table 1** Load bearing capacities and amounts of reinforcement.

8 **Table 2** The finite elements used for the representation of the two types of slabs.

9 **Table 3** Comparison of numerically obtained temperatures in the composite slab with those  
10 obtained applying the recommendations of Eurocode 4.

11 **Table 4** Fire resistance time

12 **Table 5** Measured mechanical properties of steel and concrete at room temperature (Test No. 2  
13 of [14]).

14 **Fig. 1** The two systems under study in this paper and the corresponding cross-sections: a) simply  
15 supported slab, b) the two-span continuous composite slab.

16 **Fig. 2** Temperatures at the upper and the lower sides of the composite slab and the ISO fire  
17 curve.

18 **Fig. 3** Calculation of the sagging and hogging moment resistances according to Eurocode 4.

19 **Figure 4** Evolution of the resistance moment at the mid-span of the simply supported slab with  
20 time.

21 **Fig. 5** Bending rigidity –moment curves of the slab's cross section at characteristic instants of  
22 the fire exposure

23 **Fig. 6** Flowchart for the calculation of the fire resistance according to the simplified method.

24 **Fig. 7** Evolution of the resistances and the design bending moments with time (continuous slab).

25 **Fig. 8** Moment diagrams and resistances for continuous slab in characteristic temperatures  
26 (moments given in kNm/m).

27 **Fig. 9** Simplification of the analysis model.

28 **Fig. 10** Boundary conditions that are used for the symmetry (not in scale): a) simply supported  
29 beam b) continuous beam.

30 **Fig. 11** Connection of solid elements with shell and frame elements.

31 **Fig. 12** The thermal boundary conditions.

32 **Fig. 13** Variation of the temperature in characteristic cross-section points with time.

33 **Fig. 14** Temperature distribution in the slab cross-section at 60 minutes.

34 **Fig. 15** Development of mean temperature of the lower flange of the steel sheeting with time.

35 **Fig. 16** Development of mean temperature of the web of the steel sheeting with time

36 **Fig. 17** Development of the maximum vertical displacement with time.

37 **Fig. 18** Development of the deflection rate with time.

38 **Fig. 19** The deformed shape of the continuous composite slab and the corresponding cracking  
39 strains; a) at the 30<sup>th</sup> minute, b) at the 67<sup>th</sup> minute.

40 **Fig. 20** The deformed shape of the continuous composite slab and the corresponding cracking  
41 strains; a) at 60<sup>th</sup> minute, b) at 120<sup>th</sup> minute, c) at 180<sup>th</sup> minute.

42 **Fig. 21** The test specimen and the arrangement of the loading (test No. 2 of [14]).

43 **Fig. 22** The cross section of the slab (all the dimensions in mm).

44 **Fig. 23** The positions of the thermocouples.

1  
2  
3  
4  
5  
6  
7  
8  
9  
10  
11  
12  
13  
14  
15  
16  
17  
18  
19  
20  
21  
22  
23  
24  
25  
26  
27  
28  
29  
30  
31  
32  
33  
34  
35  
36  
37  
38  
39  
40  
41  
42  
43  
44  
45  
46  
47  
48  
49  
50  
51  
52  
53  
54  
55  
56  
57  
58  
59  
60  
61  
62  
63  
64  
65

**Fig. 24** Measured and calculated temperatures in the slab.

**Fig. 25** Development of mid-span deflection with time. Comparison between numerical and test results.

Figure 1

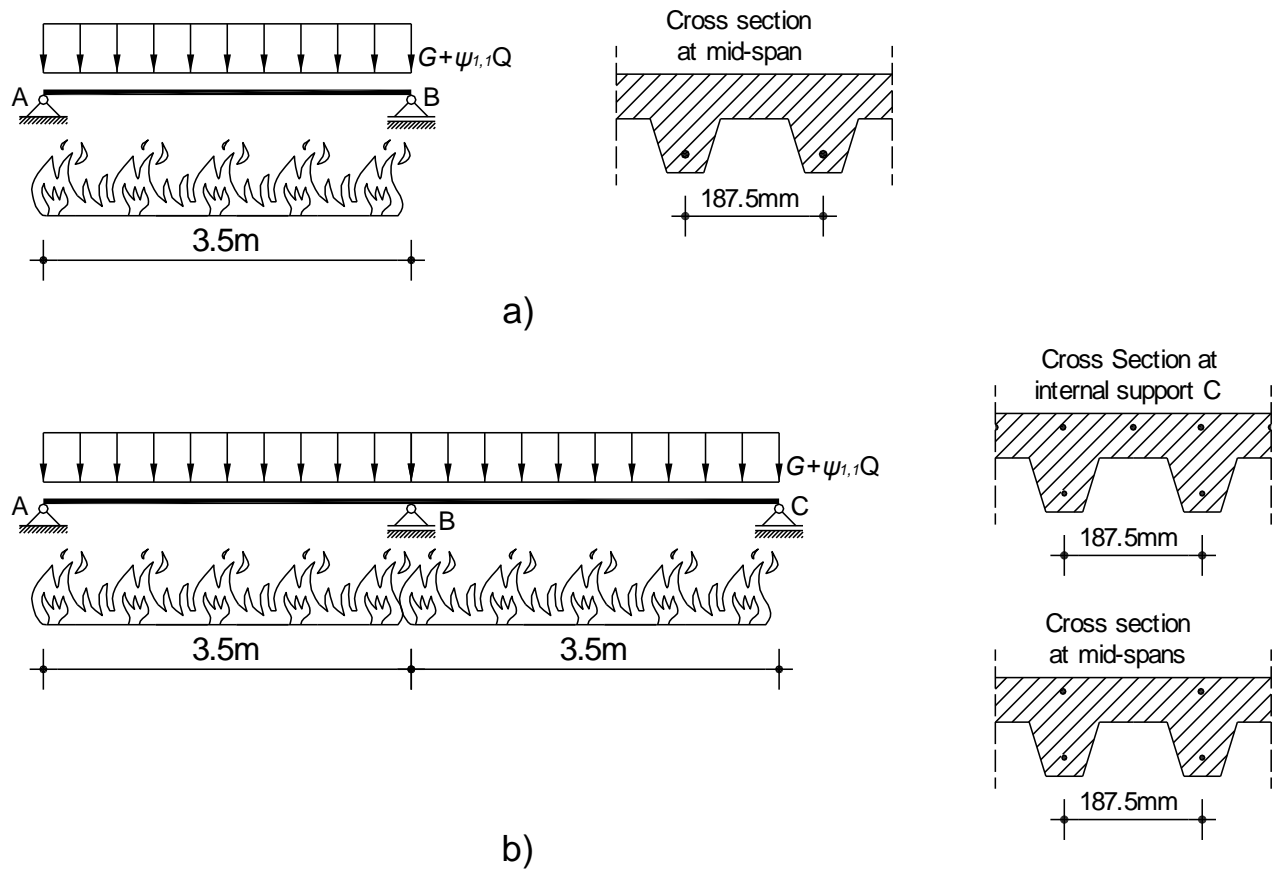


**Fig. 1** The two systems examined and the corresponding cross-sections: a) simply supported slab, b) two-span continuous composite slab

Figure 2

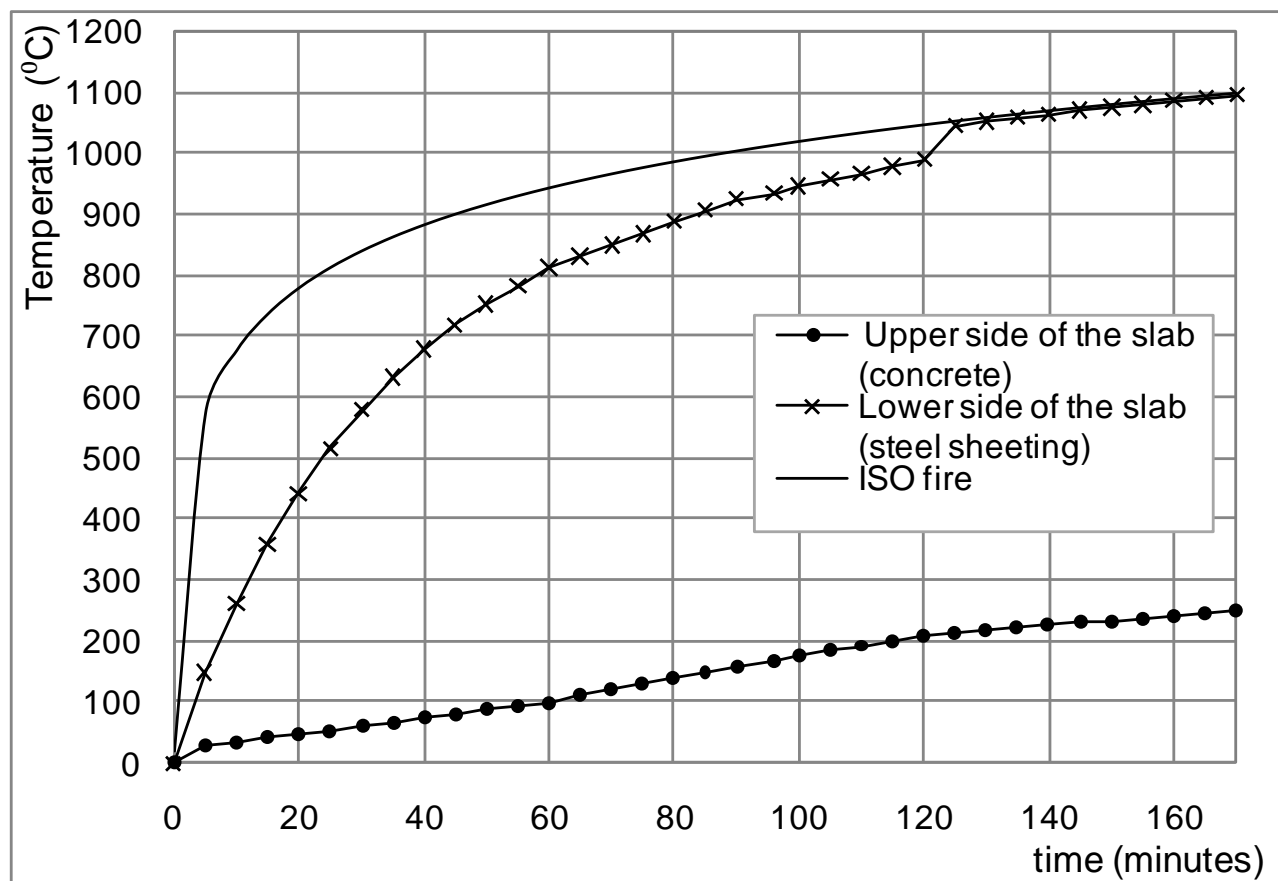
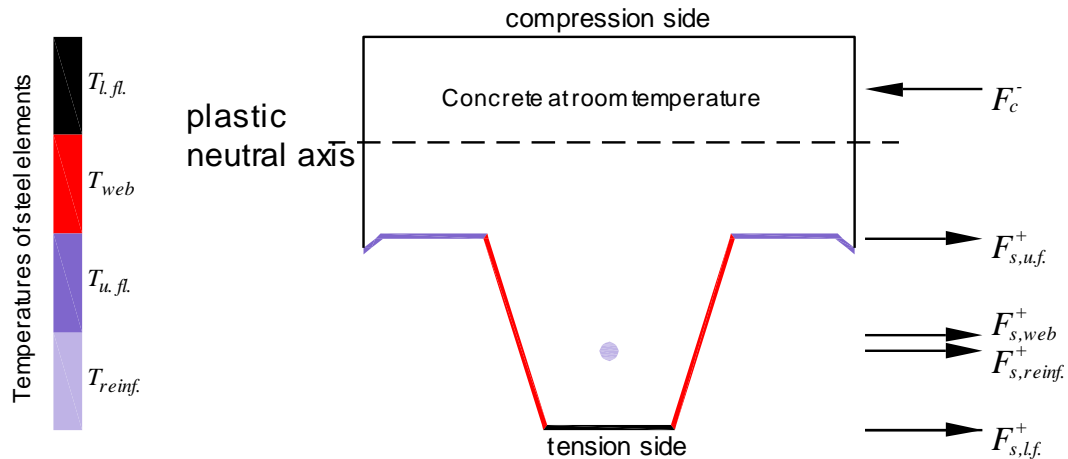


Fig. 2 Temperatures at the upper and the lower sides of the composite slab and the ISO fire curve.

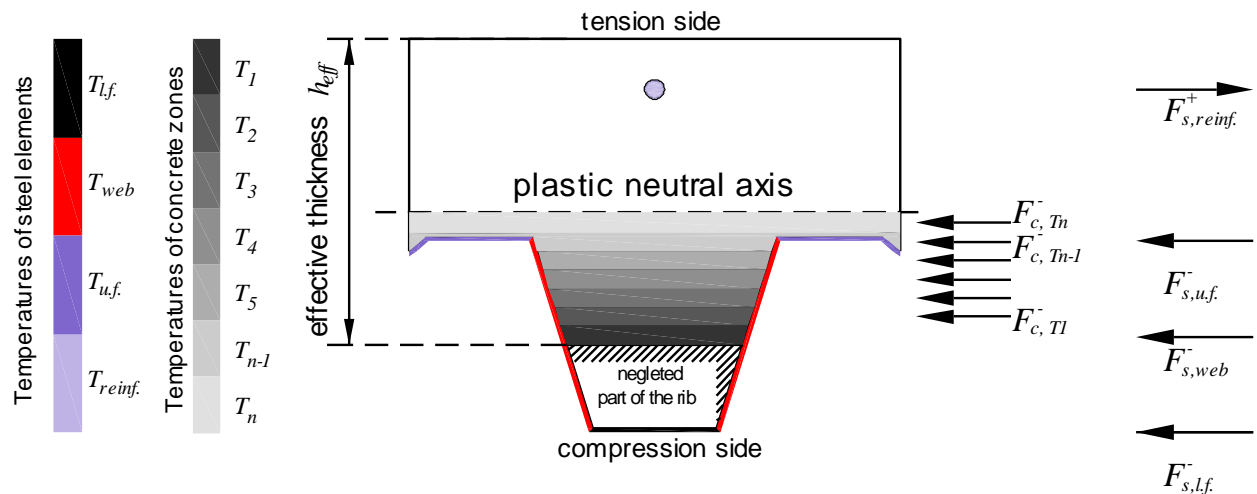
a) Sagging moments



Notes:

1. Concrete under tension is ignored due to the low tensile strength of concrete
2. The upper reinforcement is ignored due to the low contribution to the resistance moment

b) Hogging moments



Notes:

1. Concrete under tension is ignored due to the low tensile strength of concrete
2. The lower reinforcement is ignored due to the low contribution to the resistance moment
3. Concrete with temperature greater than  $T_l$  is ignored

Fig. 3 Calculation of the sagging and hogging moment resistances according to Eurocode 4.

Figure 4

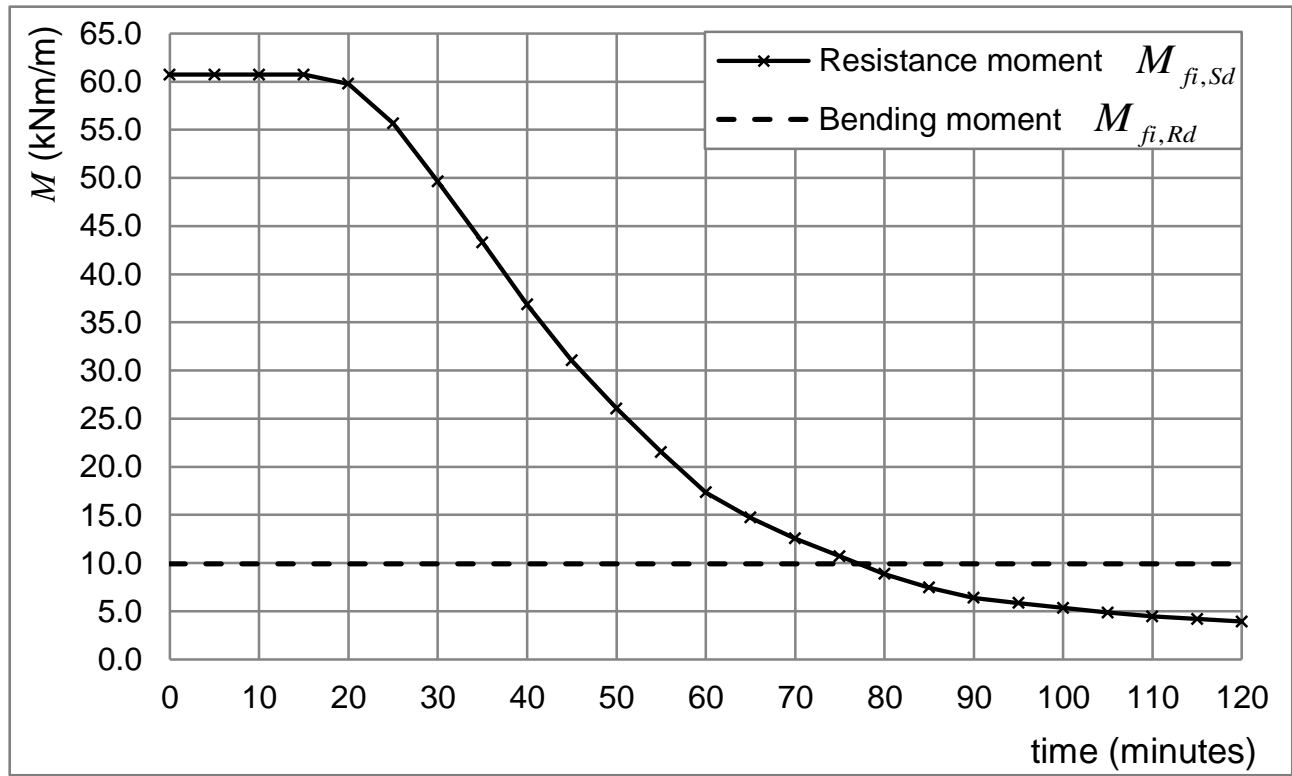
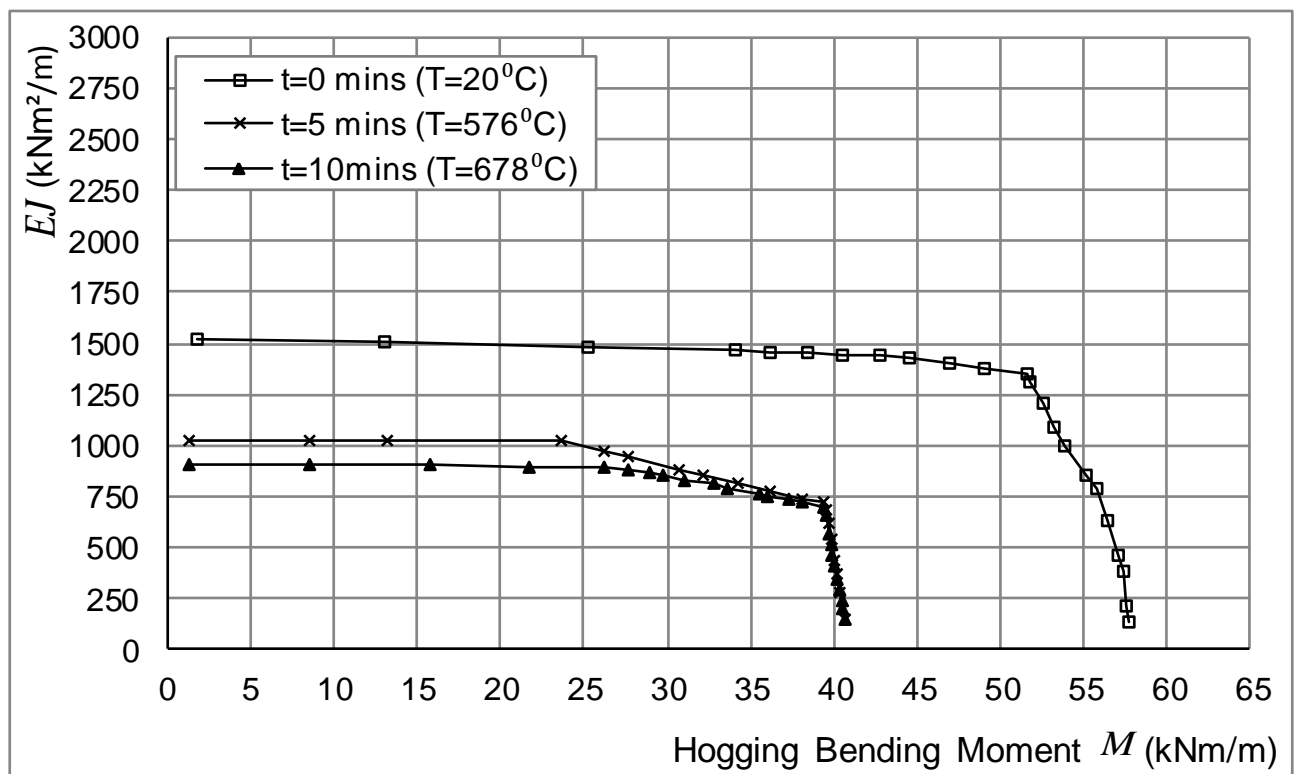
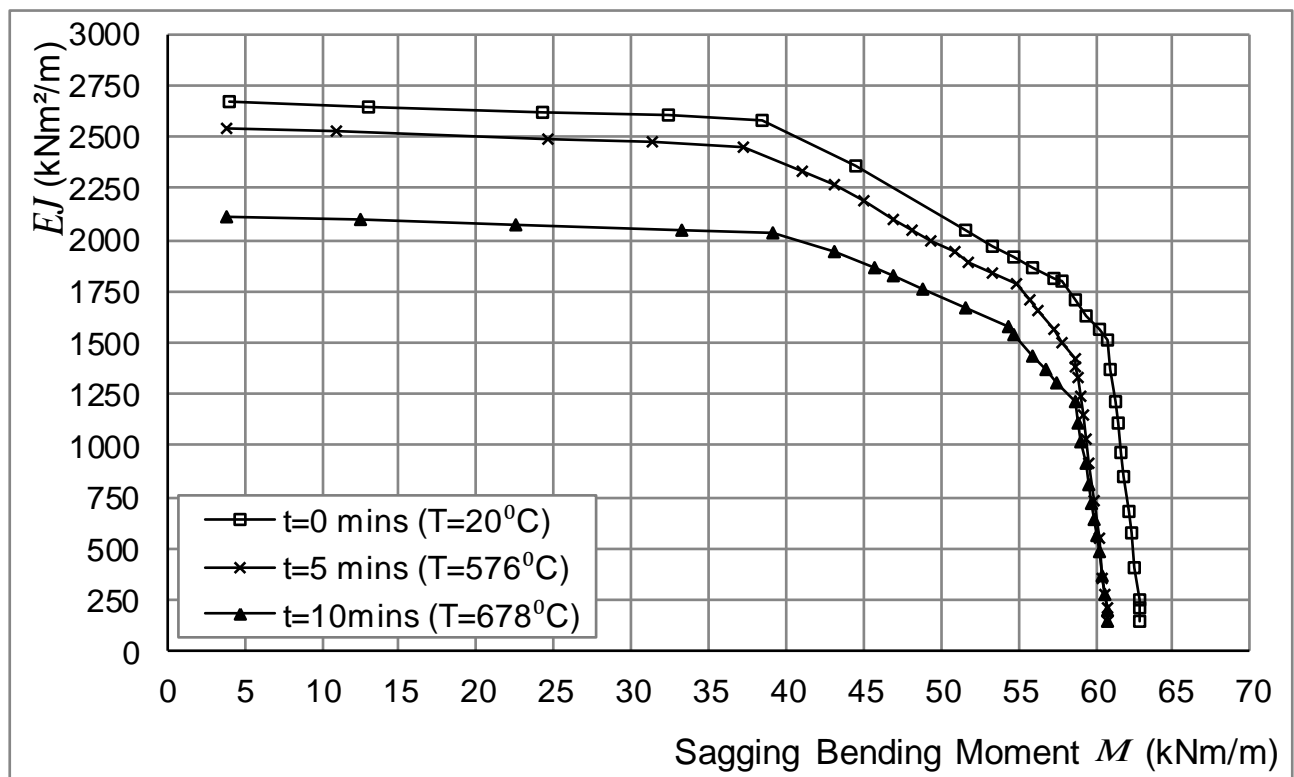


Fig. 4 Evolution of the resistance moment at the mid-span of the simply supported slab with time.



Figure 5



**Fig. 5** Bending rigidity –moment curves of the cross section of the slab at characteristic instants of the fire exposure:

a) sagging bending moment b) hogging bending moment

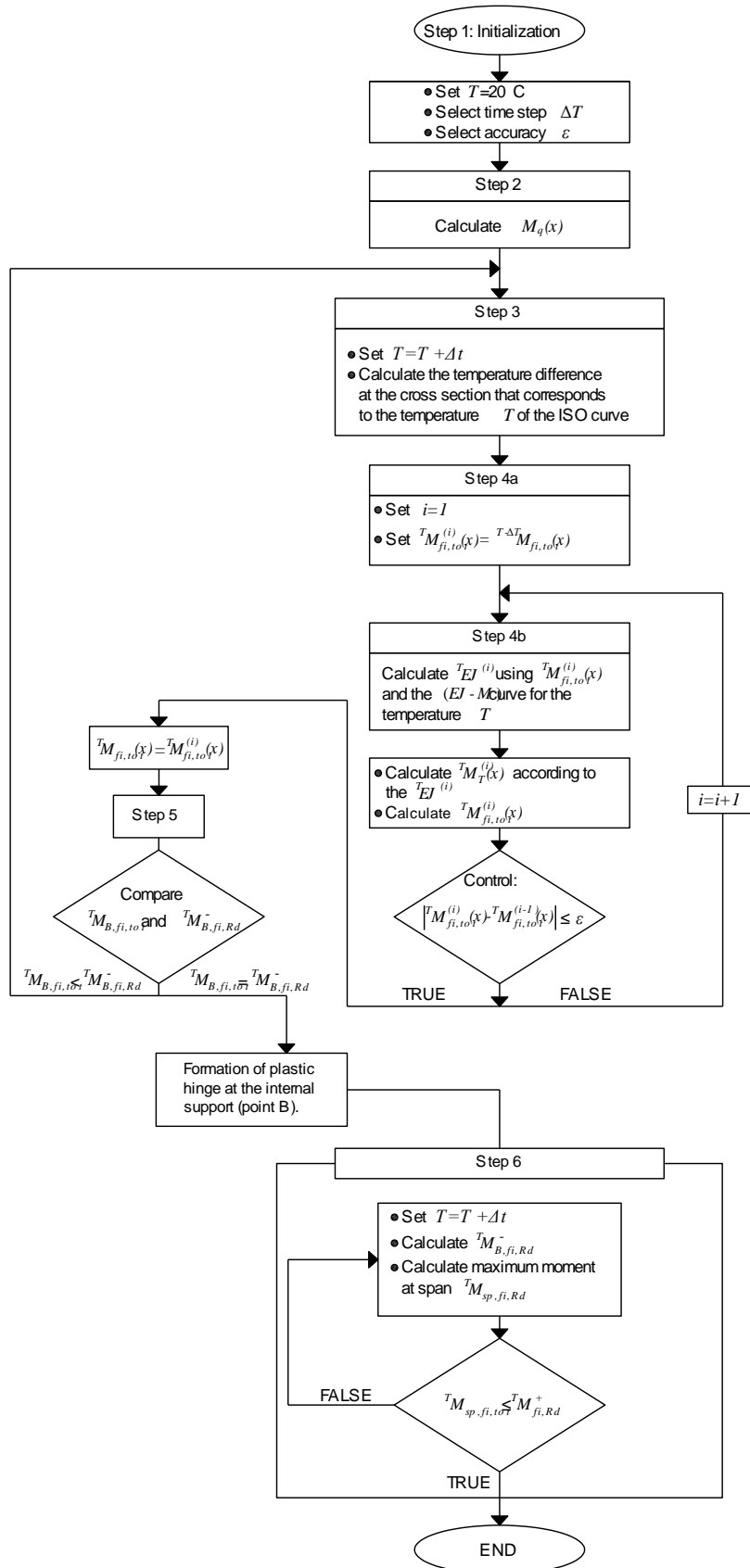


Fig. 6 Flowchart for the calculation of the fire resistance according to the simplified method.

Figure 7

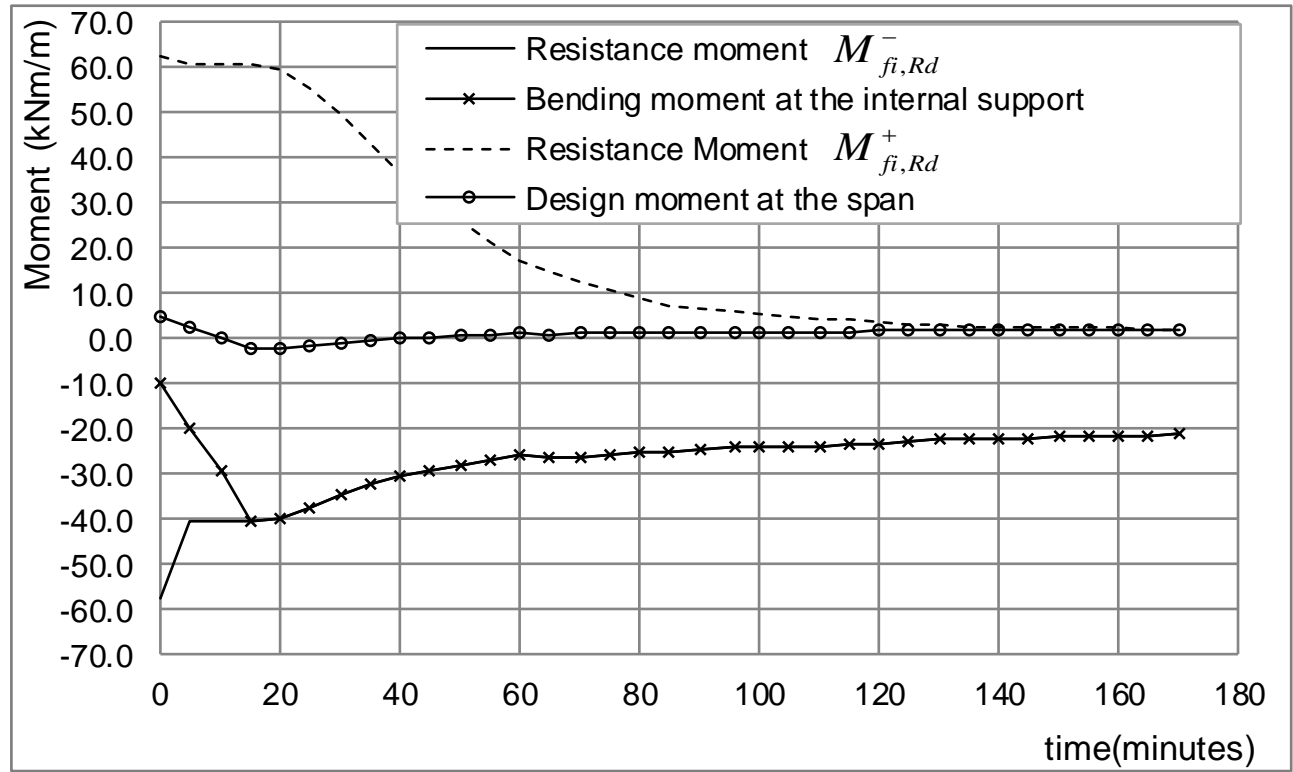
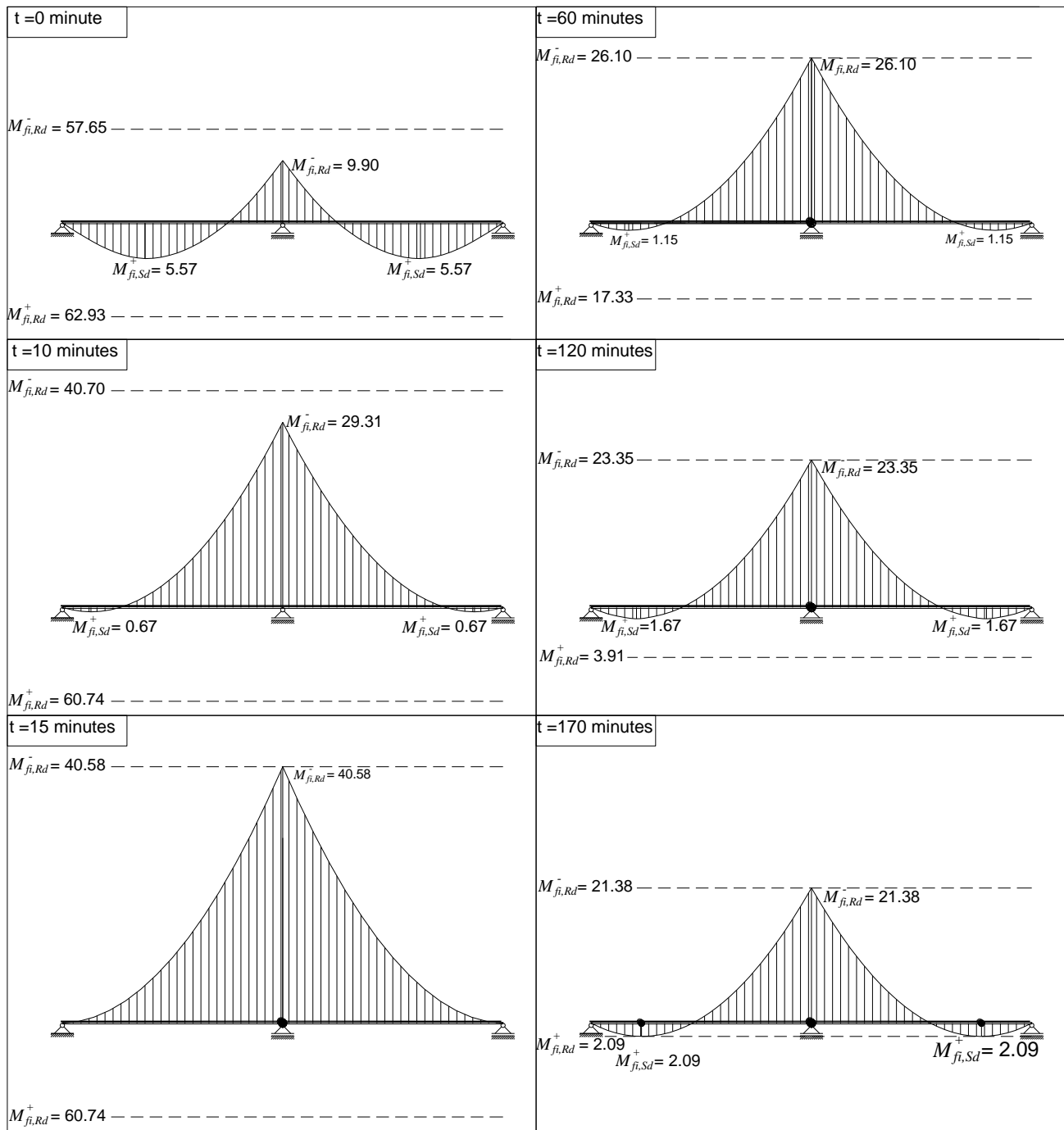
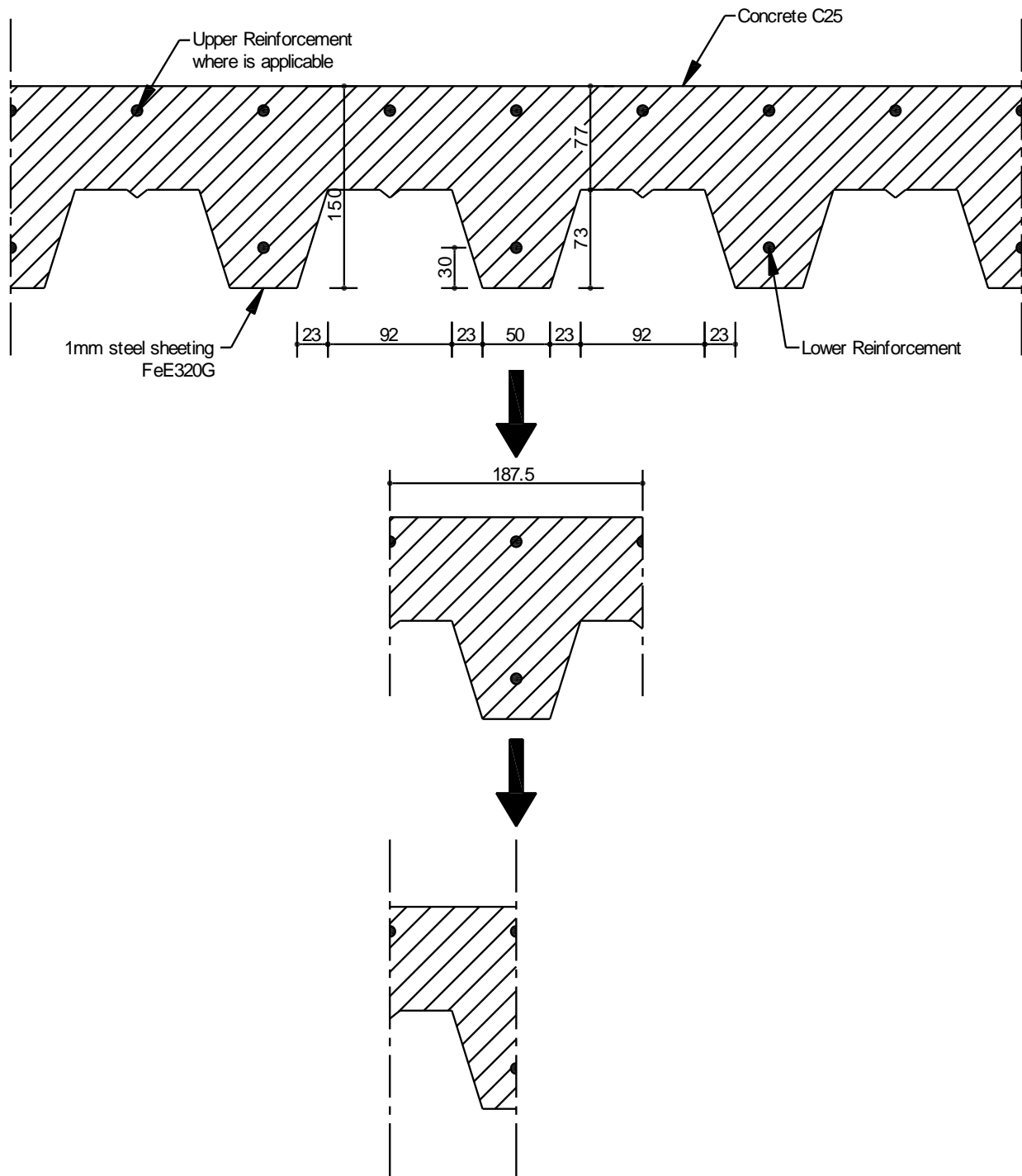


Fig. 7 Evolution of the design bending moments and the corresponding resistances with time (continuous slab).



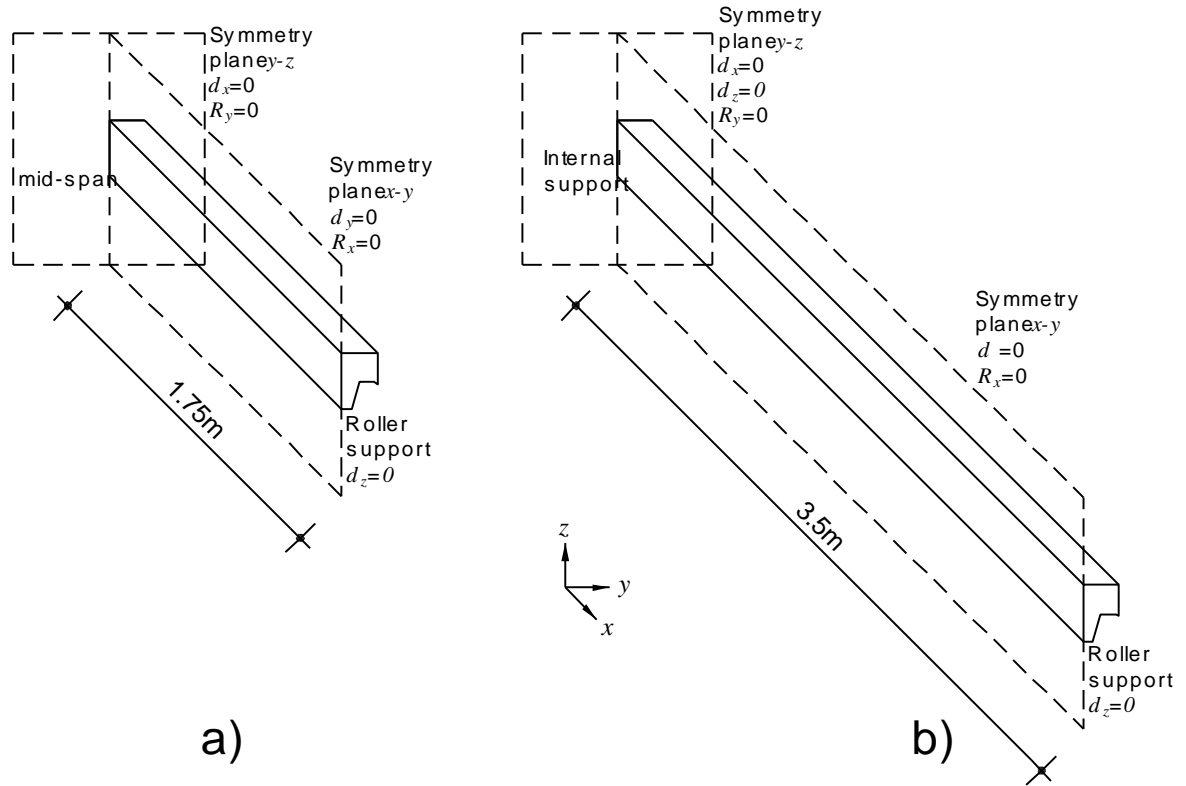
**Fig. 8** Moment diagrams and resistances for continuous slab in characteristic temperatures (moments given in kNm/m).

Figure 9



**Fig. 9** Simplification of the analysis model.

Figure 10



**Fig. 10** Boundary conditions that are used for the numerical model (not in scale): a) simply supported beam b) continuous beam.

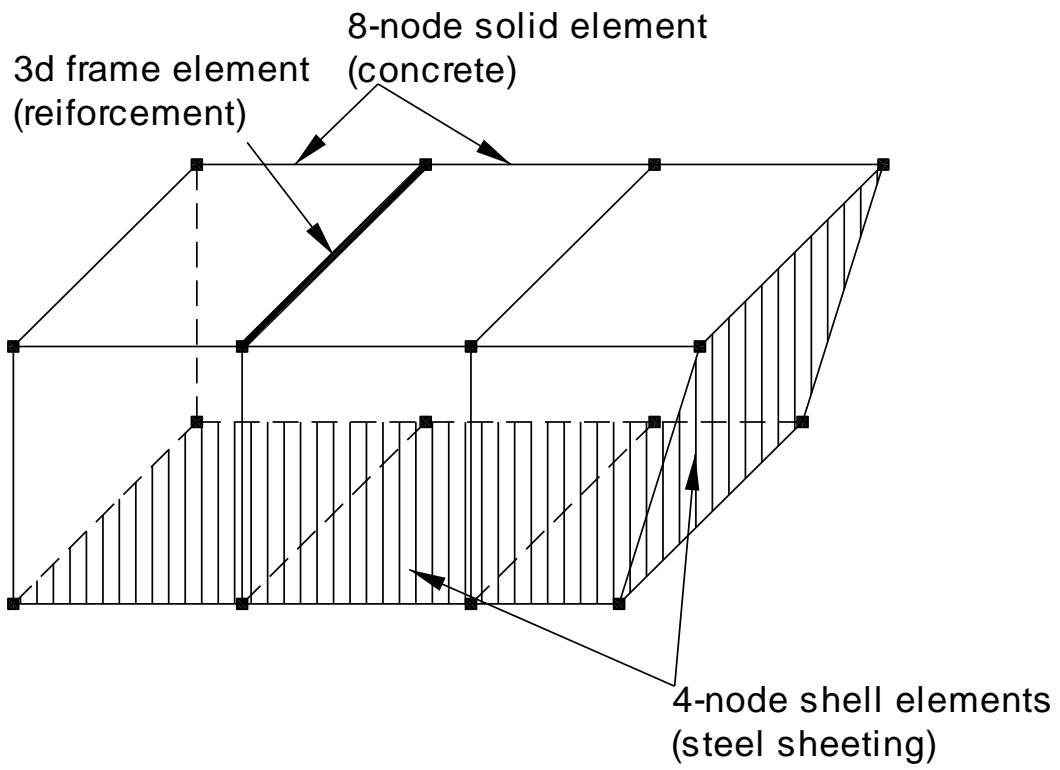


**Fig.11** Connection of solid elements with shell and frame elements.

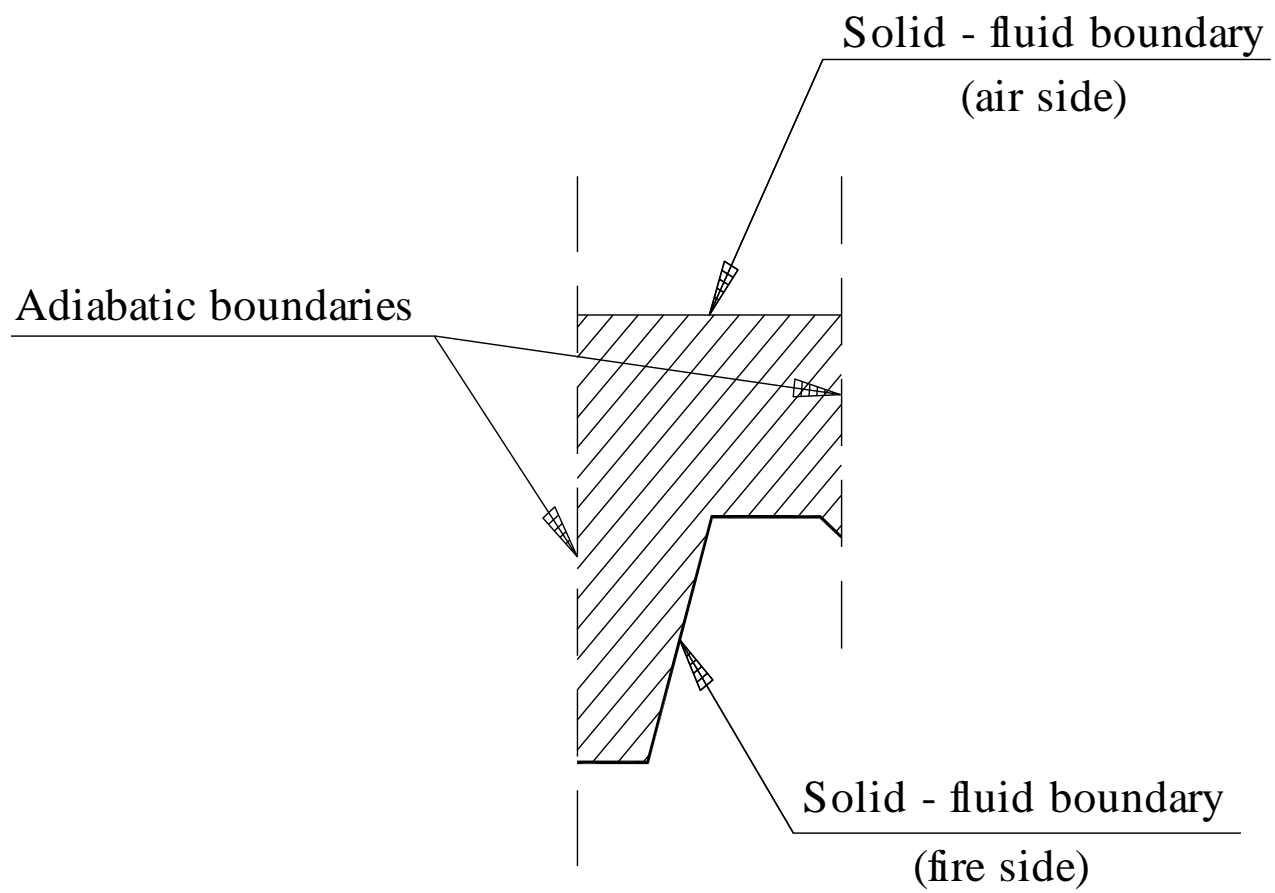


**Fig. 12** The thermal boundary conditions.



Figure 13

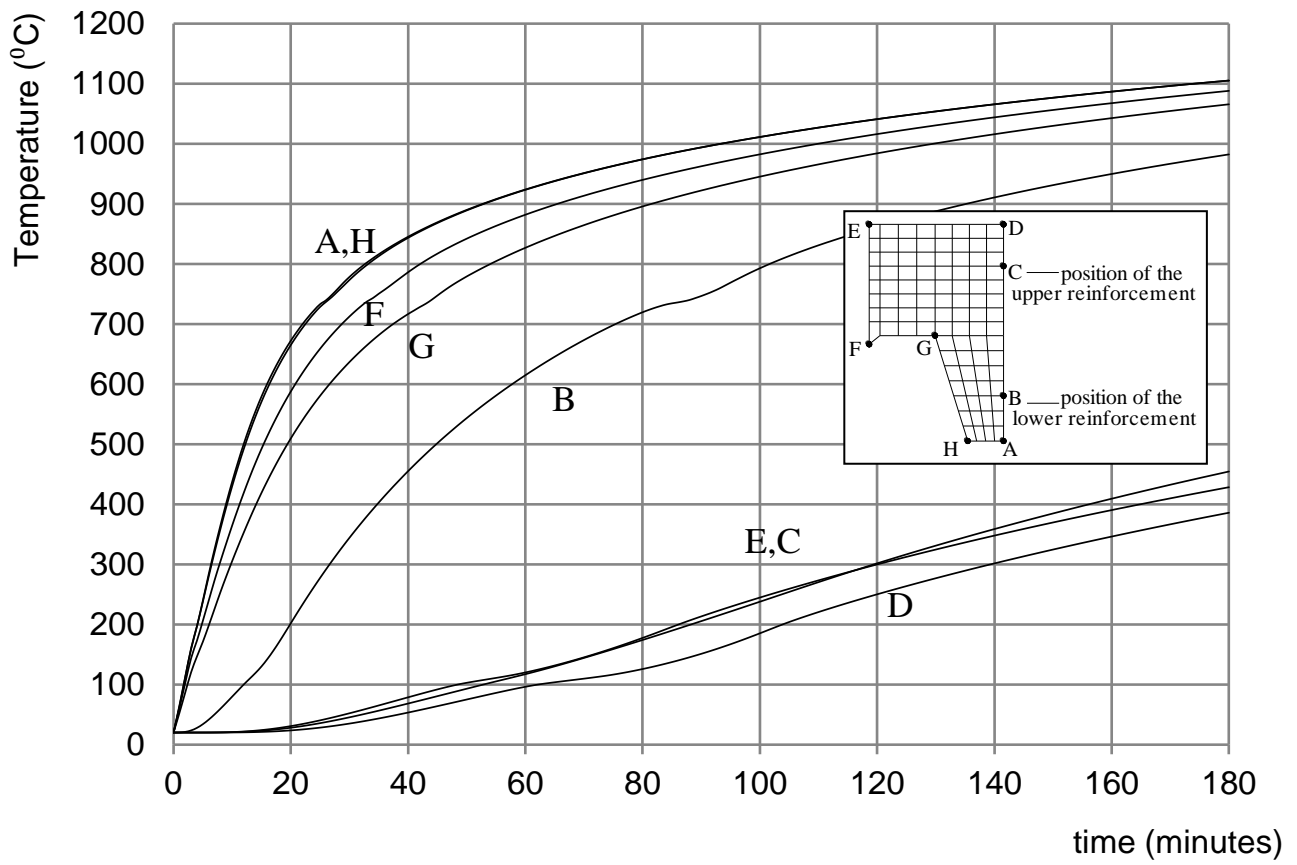
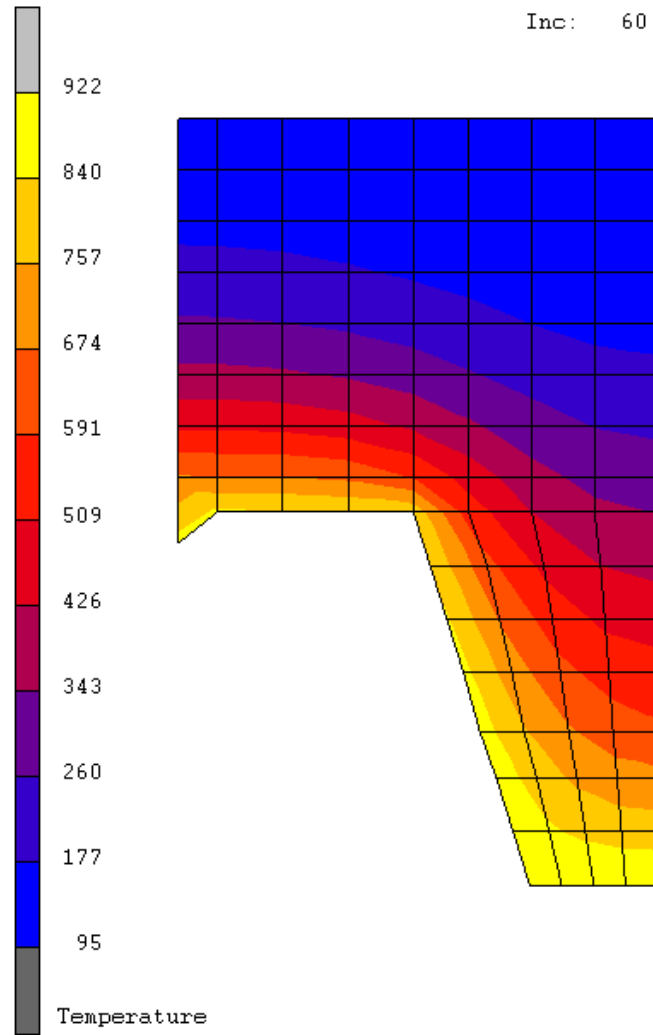
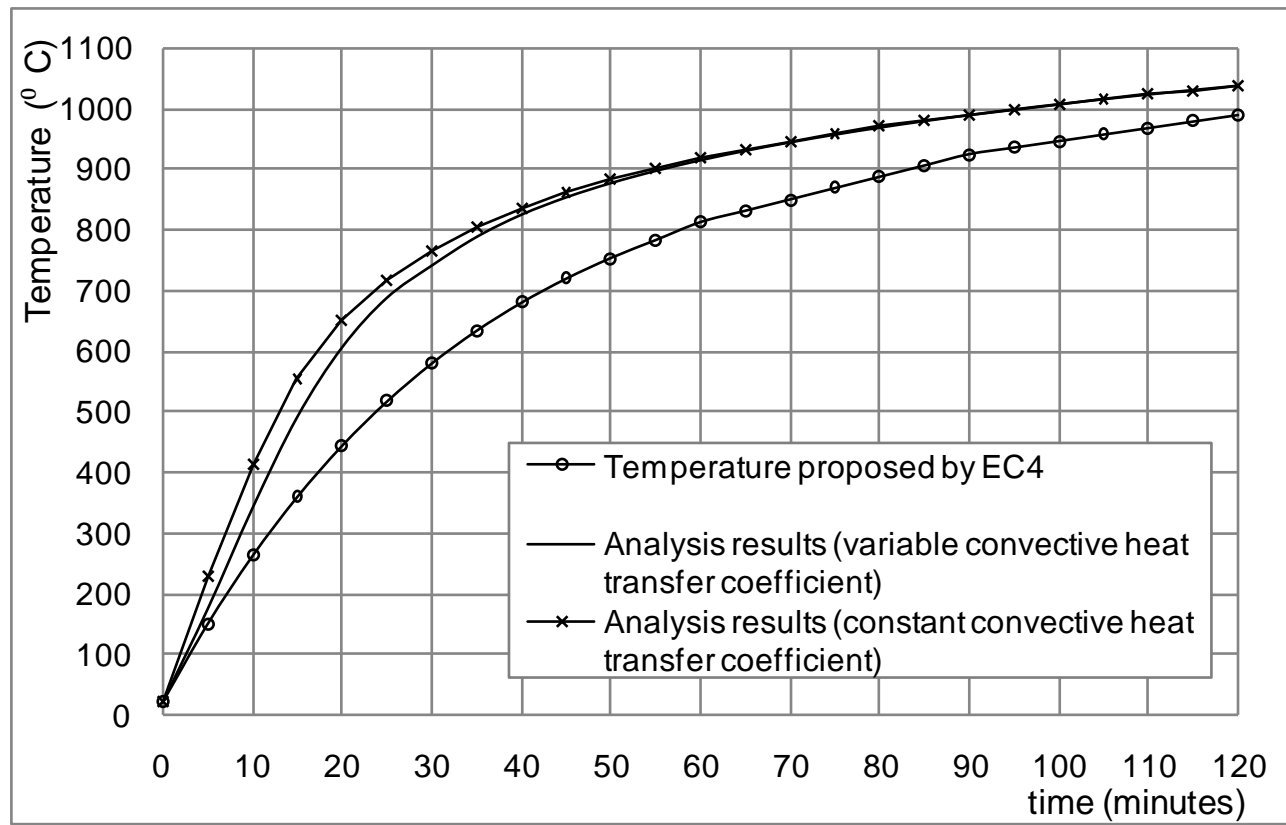


Fig. 13 Variation of the temperature in characteristic cross-section points with time.



**Fig. 14** Temperature distribution in the slab cross-section at the 60<sup>th</sup> minute.



**Fig. 15** Development of mean temperature of the lower flange of the steel sheeting with time.

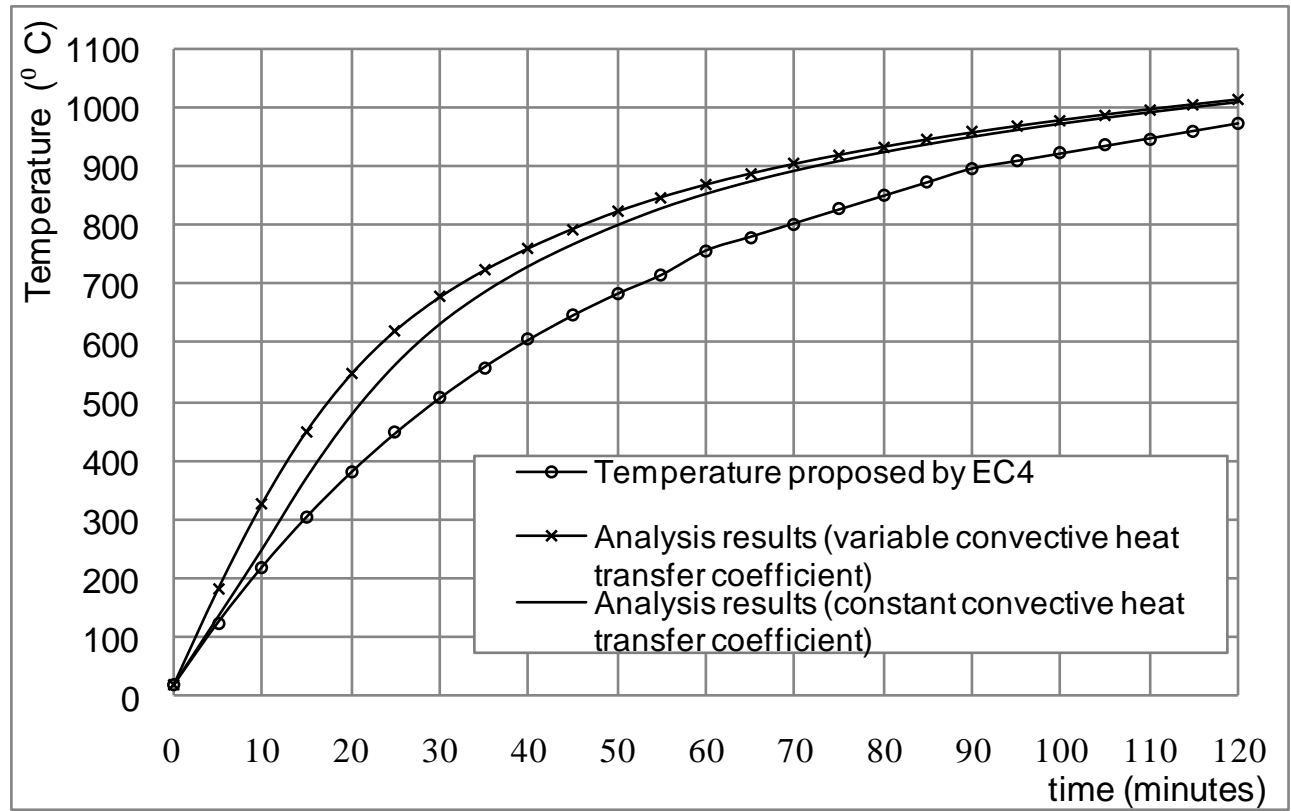


**Fig. 16** Development of mean temperature of the web of the steel sheeting with time.

Figure 17

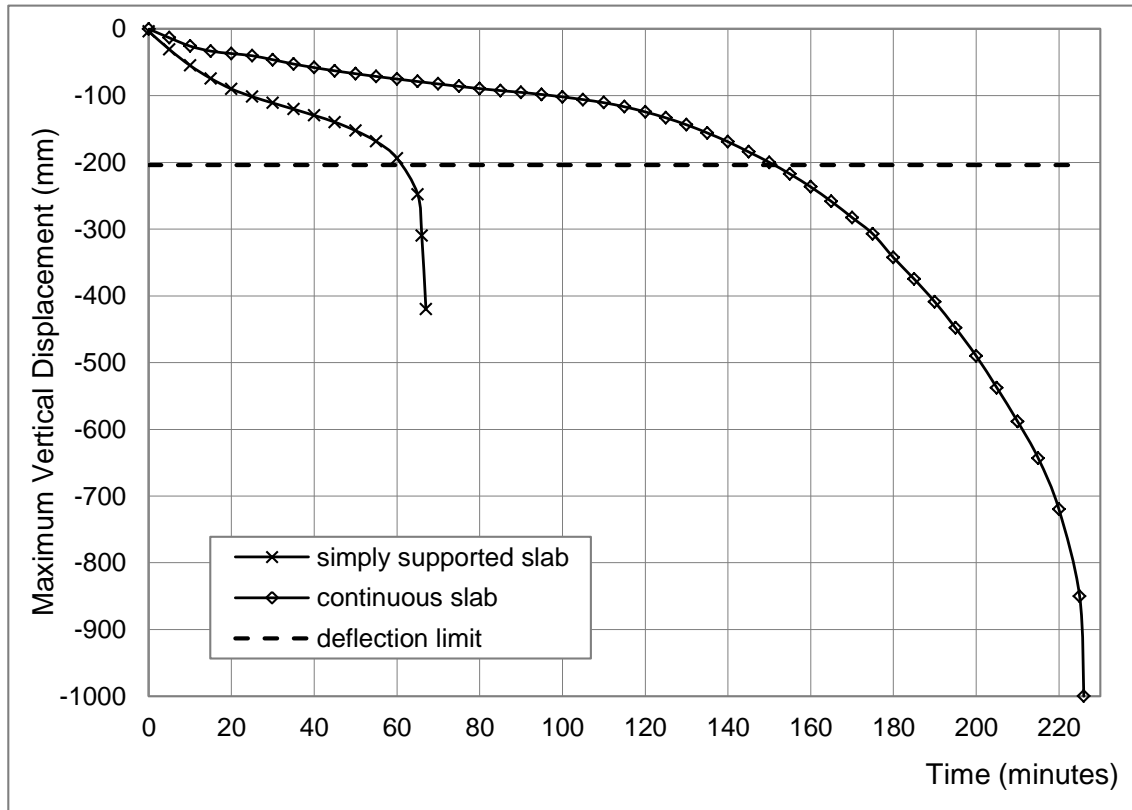


Fig. 17 Development of the maximum vertical displacement with time.

Figure 18

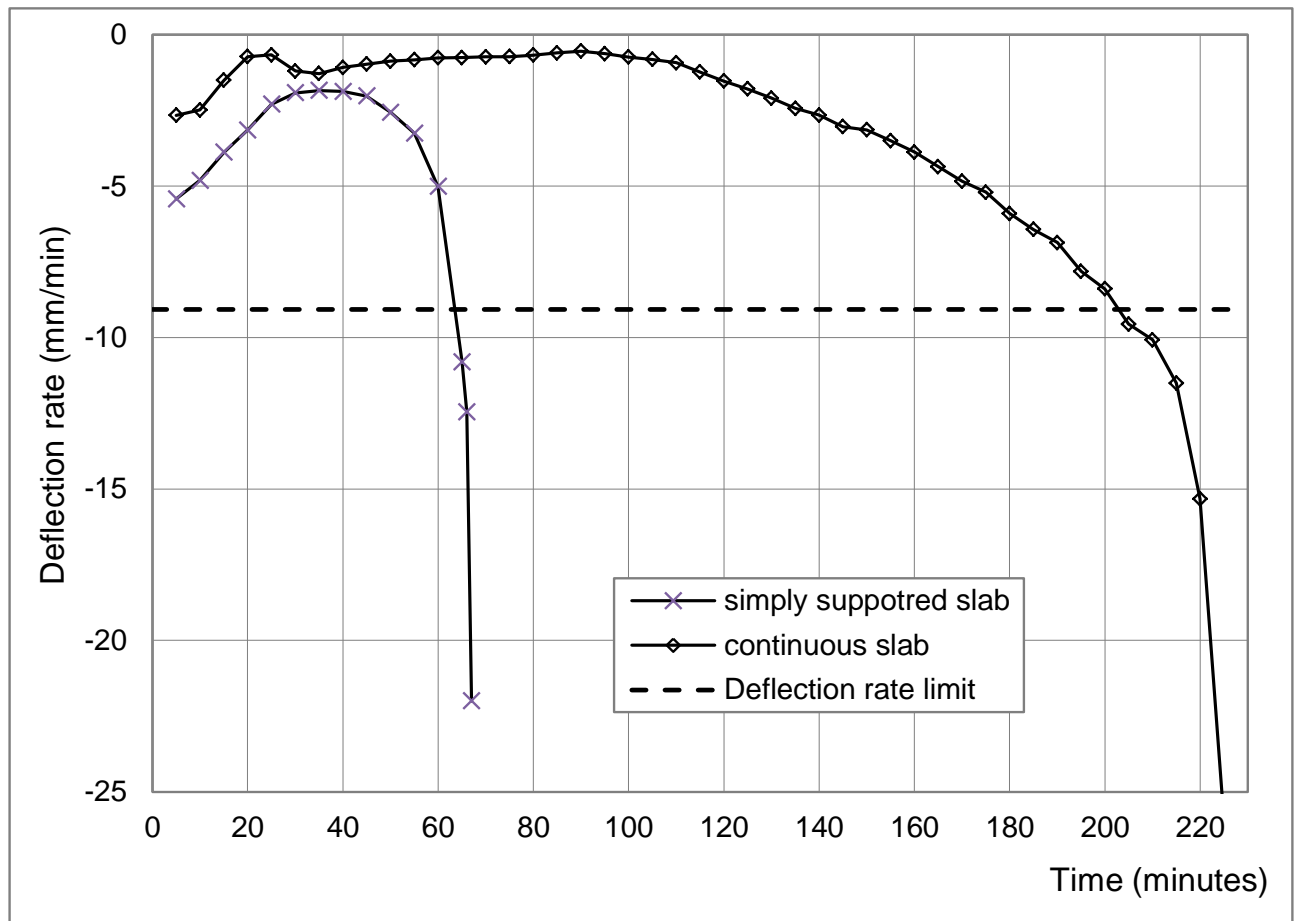
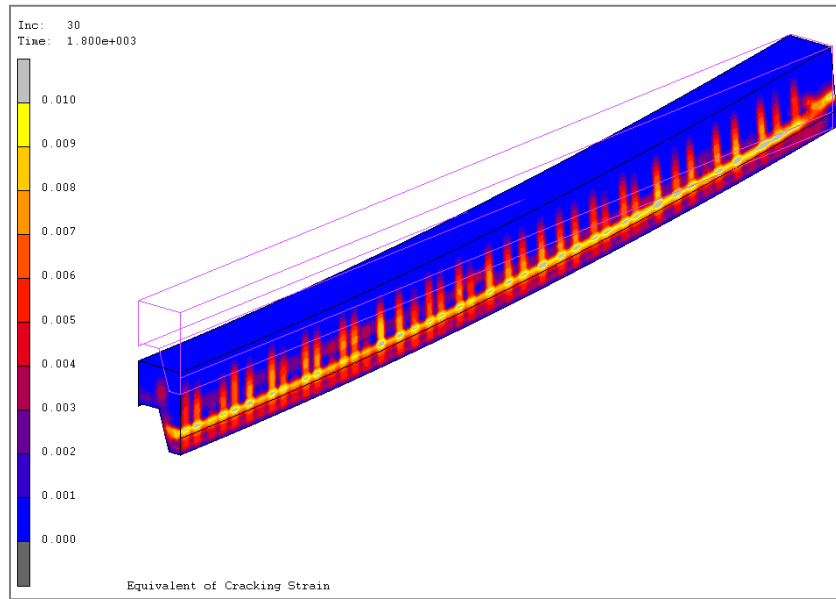
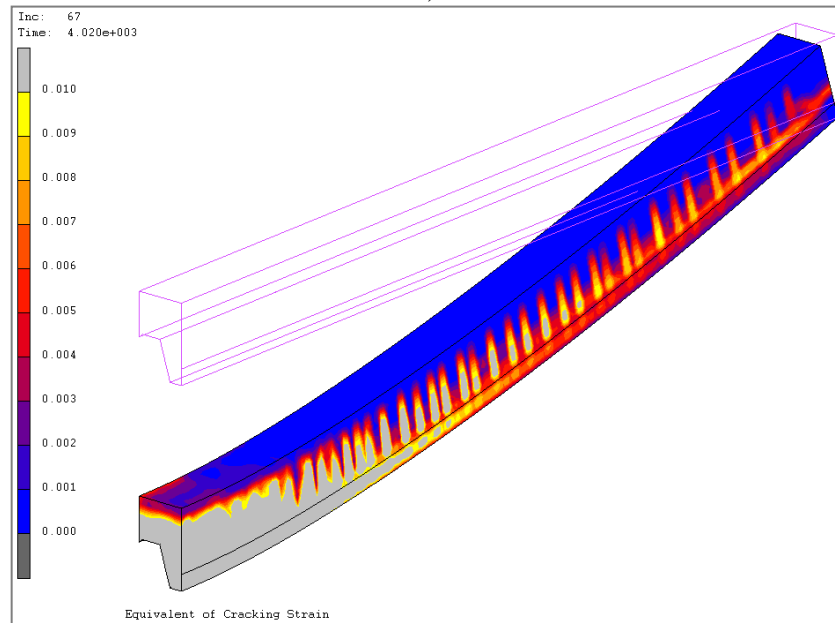


Fig. 18 Development of the deflection rate with time.

Figure 19



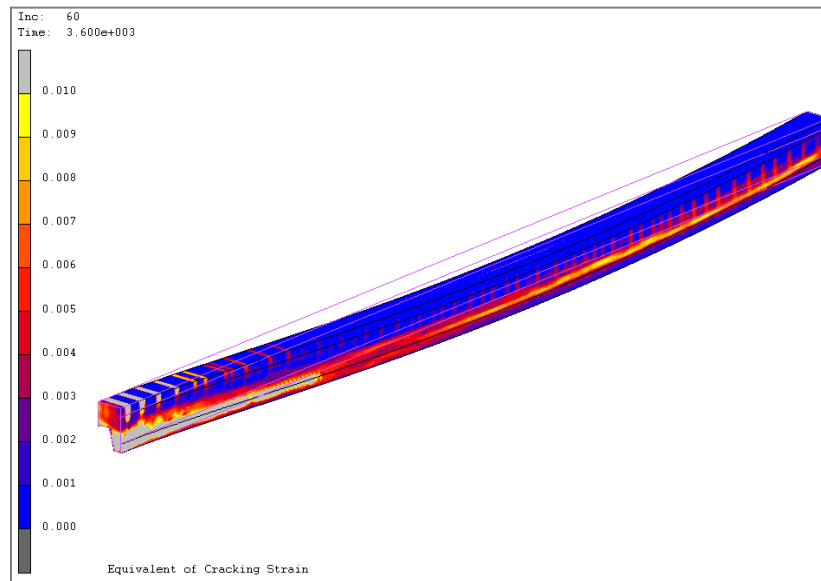
a)



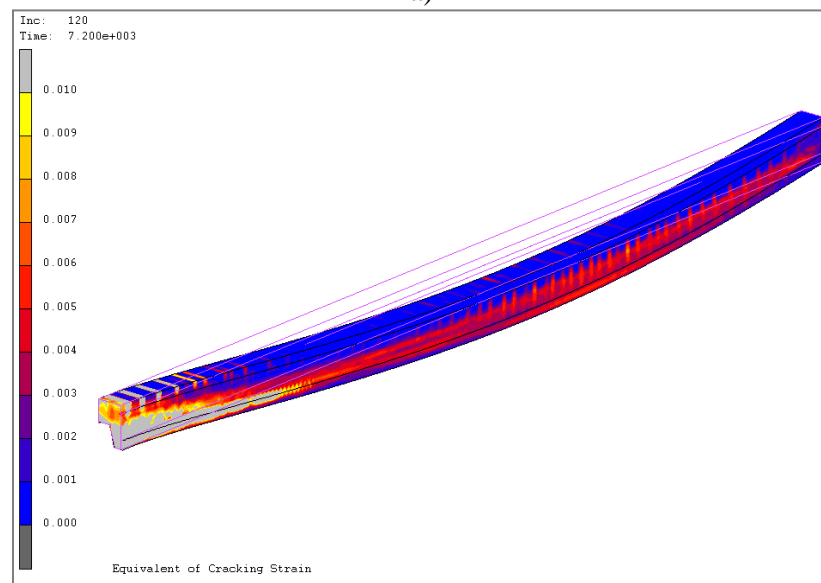
b)

**Fig. 19** The deformed shape of the continuous composite slab and the corresponding cracking strains; a) at the 30<sup>th</sup> minute, b) at the 67<sup>th</sup> minute.

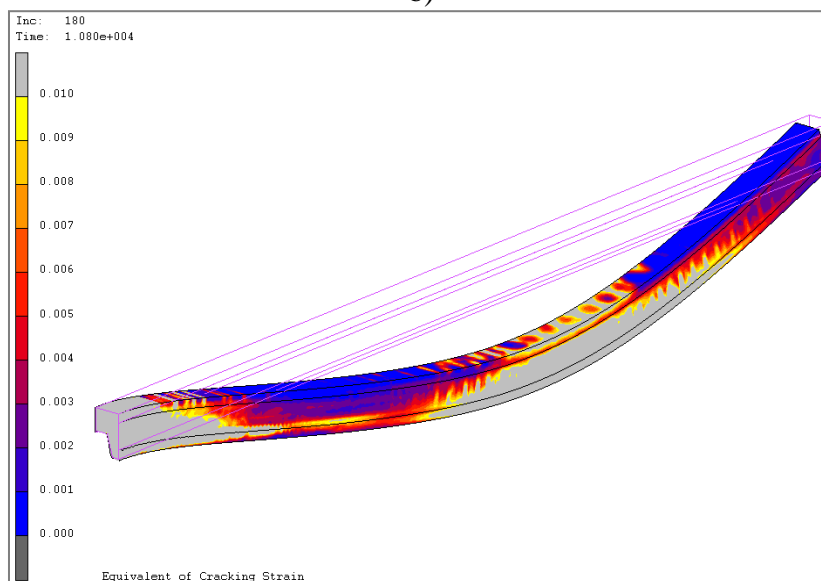
Figure 20



a)



b)



c)

**Fig. 20** The deformed shape of the continuous composite slab and the corresponding cracking strains; a) at 60<sup>th</sup> minute, b) at 120<sup>th</sup> minute, c) at 180<sup>th</sup> minute.



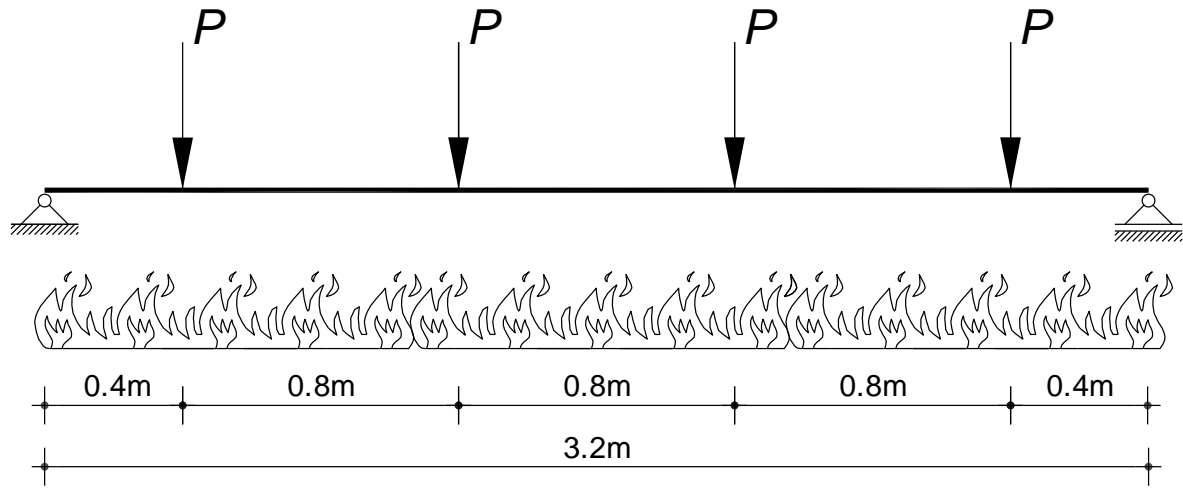


**Fig. 21** The test specimen and the arrangement of the loading (test No. 2 of [14]).

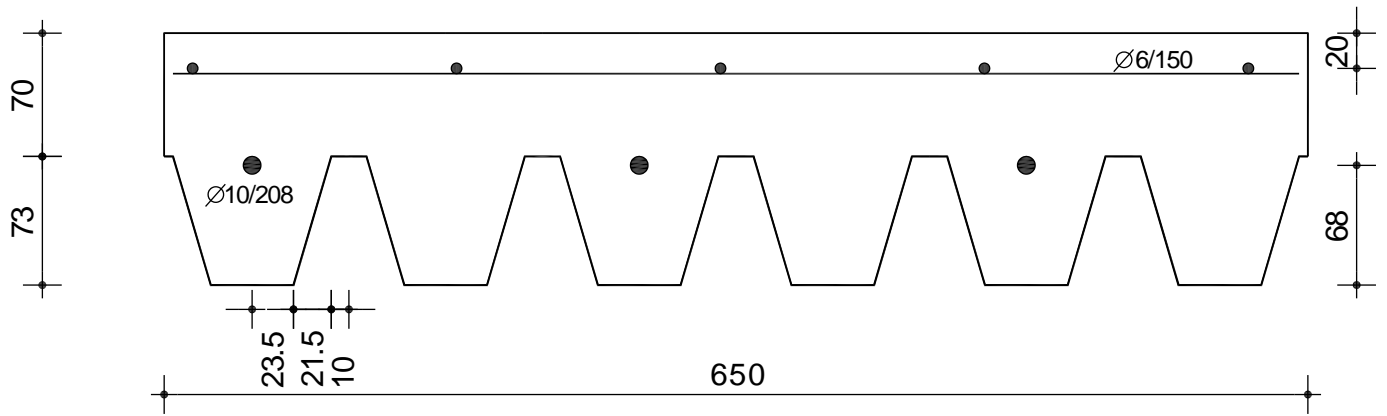


**Fig. 22** The cross section of the slab (all the dimensions in mm)

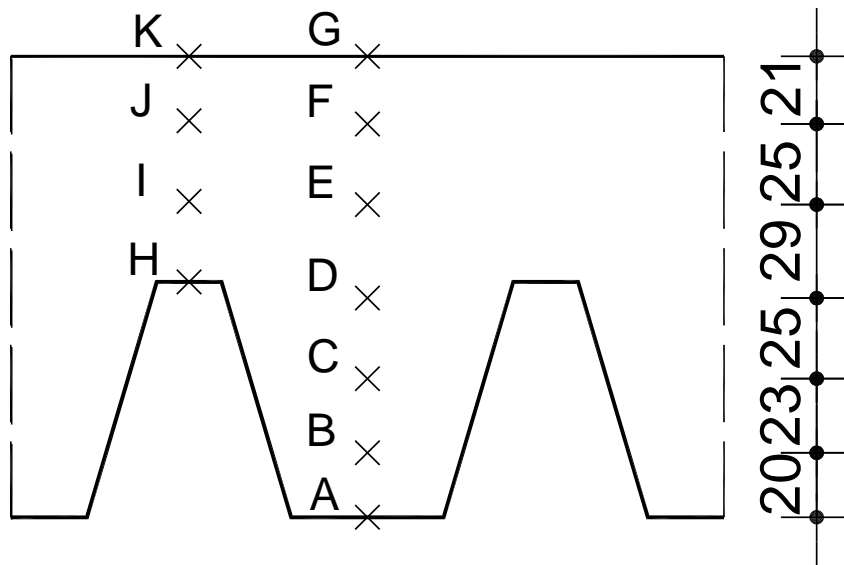
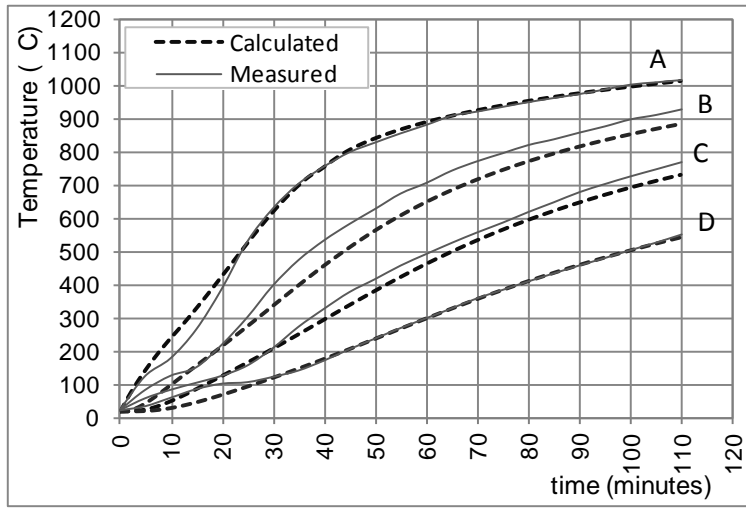
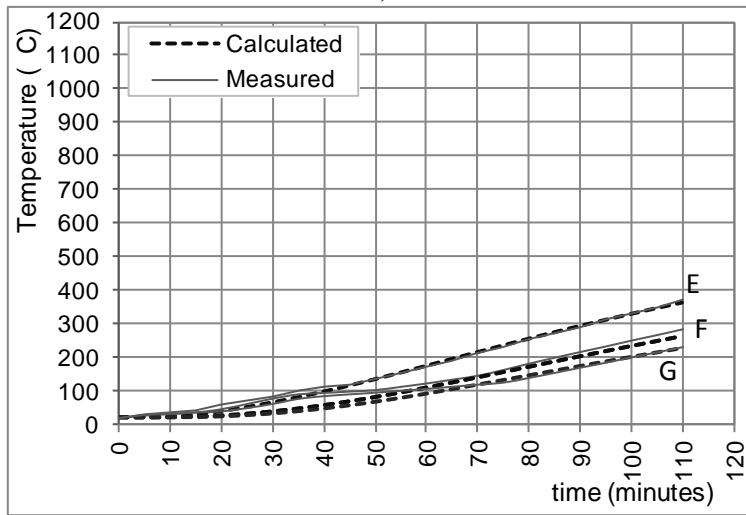


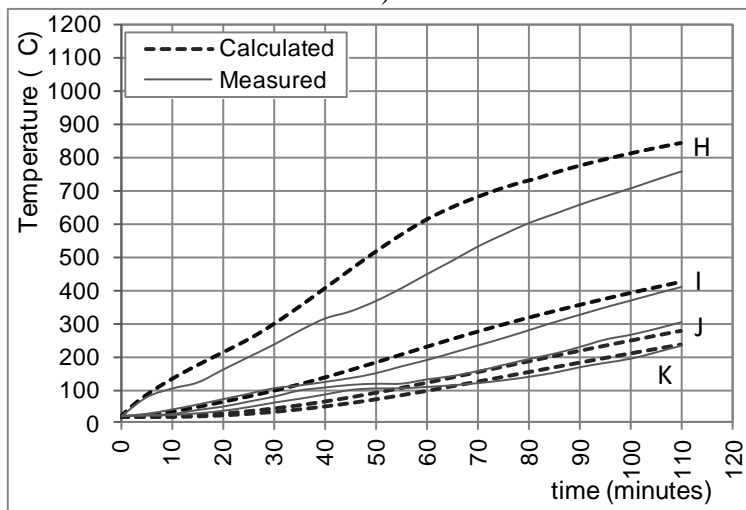
**Fig. 23** The positions of the thermocouples.



a)



b)



c)

Fig. 24 Measured and calculated temperatures in the slab.

Figure 25

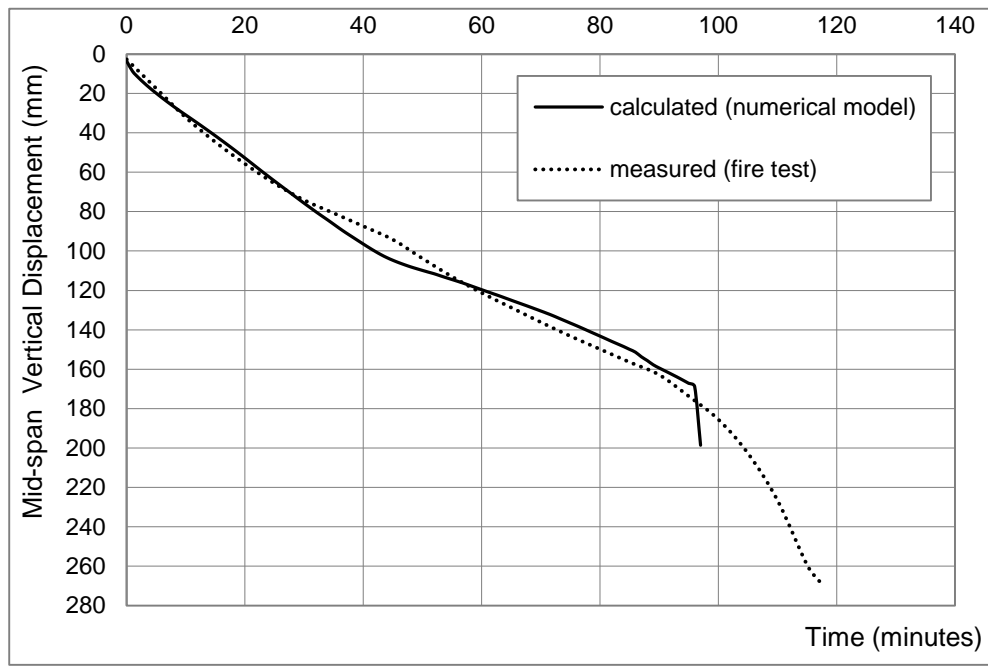


**Fig. 25** Development of mid-span deflection with time. Comparison between numerical and test results.

**Table 1** Load bearing capacities and amounts of reinforcement.

	$M_{Rd}^+$ kN·m/m	$M_{Rd}^-$ kN·m/m	Lower reinf.	Upper reinf.	<i>Strength utilization factor <math>\lambda</math></i>
Simply supported	62.72	-	Ø8/187.5	-	0.314
Continuous slab	62.93	57.65	Ø8/187.5	Ø12/120	0.341

**Table 2** The finite elements used for the representation of the two types of slabs.

	Solid elements (concrete)	Shell elements (steel sheeting)	Frame elements (reinforcement)
Simply supported slab	13300	2625	175
Continuous slab	32200	5250	700

**Table 3** Comparison of numerically obtained temperatures in the composite slab with those obtained applying the recommendations of Eurocode 4.

		Mean temperature in the numerical model ( $^{\circ}$ C)	Eurocode 4 procedure ( $^{\circ}$ C)	Difference (%)
60 minutes	Lower Flange	924.368	812.973	13.70
	Web	879.262	757.178	16.12
	Upper Flange	856.877	694.389	23.40
	Lower Reinforcement	614.768	571.409	7.59
90 minutes	Lower Flange	994.437	925.316	7.47
	Web	964.330	896.351	7.58
	Upper Flange	943.801	840.145	12.34
	Lower Reinforcement	746.638	743.480	0.42
120 minutes	Lower Flange	1041.374	989.946	5.20
	Web	1018.830	973.045	4.71
	Upper Flange	1001.067	924.332	8.30
	Lower Reinforcement	861.595	844.705	2.00



**Table 4** Comparison of the fire resistance times

	Simply supported slab	Continuous slab
Simplified model	77 minutes	170 minutes
Advanced calculation model- strength	67 minutes	226 minutes
Advanced calculation model- Deflection limit criterion	62 minutes	152 minutes
Advanced calculation model -Rate of deflection criterion	62 minutes	203 minutes

**Table 5** Measured mechanical properties of steel and concrete at room temperature (Test No. 2 of [14]).

<b>Steel</b>		
	Yield stress	Ultimate stress
Ø6 (hot-rolled)	552 MPa	598 MPa
Ø10 (cold-worked)	587 MPa	677 MPa
Steel sheeting	306 MPa	384 MPa

<b>Concrete</b>		
	Compressive stress	Tensile stress
C25	33.6 MPa	3.5 MPa